

SCALING UP TiO_2 ANODIZATION DEVICE
FOR GAS-PHASE PHOTOCATALYSIS

AHMAD LUQMANN BIN AFANDI

BACHELOR OF ENGINEERING
TECHNOLOGY (ENERGY & ENVIRONMENT)
WITH HONORS

UNIVERSITI MALAYSIA PAHANG

UNIVERSITI MALAYSIA PAHANG

DECLARATION OF THESIS AND COPYRIGHT

Author's Full Name : AHMAD LUQMANN BIN AFANDI
Date of Birth :
Title : SCALING UP ANODIC TIO₂ NANOTUBE LAYERS
FOR GAS-PHASE PHOTOCATALYSIS
Academic Session :

I declare that this thesis is classified as:

- CONFIDENTIAL (Contains confidential information under the Official Secret Act 1997)*
 RESTRICTED (Contains restricted information as specified by the organization where research was done)*
 OPEN ACCESS I agree that my thesis to be published as online open access (Full Text)

I acknowledge that Universiti Malaysia Pahang reserves the following rights:

1. The Thesis is the Property of Universiti Malaysia Pahang
2. The Library of Universiti Malaysia Pahang has the right to make copies of the thesis for the purpose of research only.
3. The Library has the right to make copies of the thesis for academic exchange.

Certified by:

(Student's Signature)

New IC/Passport Number
Date: 16 FEBRUARY 2022

(Supervisor's Signature)

ASSOC PROF. DR. AZRIHA ABD AZIZ
DEPUTY DEAN (RESEARCH & POSTGRADUATE STUDY)
FACULTY OF CIVIL ENGINEERING TECHNOLOGY
UNIVERSITI MALAYSIA PAHANG
LEBUHRAYA TUN RAZAK
26300 GAMBANG, KUANTAN, PAHANG
TEL : +609-5493002 / 2226 FAKS : +609-5492900

Name of Supervisor
Date: 16/2/2022

NOTE : * If the thesis is CONFIDENTIAL or RESTRICTED, please attach a thesis declaration letter.



SUPERVISOR'S DECLARATION

I hereby declare that I have checked this thesis and in my opinion, this thesis is adequate in terms of scope and quality for the award of the degree of Bachelor of Engineering Technology (Energy & Environment) with Honors.

(Supervisor's Signature)

Full Name : **ASSOC PROF. DR. AZRINA ABD AZIZ**
DEPUTY DEAN (RESEARCH & POSTGRADUATE STUDY)
FACULTY OF CIVIL ENGINEERING TECHNOLOGY
UNIVERSITI MALAYSIA PAHANG
LEBUHRAYA TUN RAZAK
Position : 26300 GAMBANG, KUANTAN, PAHANG
TEL : +609-5493002 / 2226 FAKS : +609-5492908
Date : 16/2/2022



STUDENT'S DECLARATION

I hereby declare that the work in this thesis is based on my original work except for quotations and citations which have been duly acknowledged. I also declare that it has not been previously or concurrently submitted for any other degree at Universiti Malaysia Pahang or any other institutions.

(Student's Signature)

Full Name : AHMAD LUQMANN BIN AFANDI

ID Number : TC18008

Date : 16 FEBRUARY 2022

SCALING UP TiO_2 ANODIZATION DEVICE FOR GAS-PHASE
PHOTOCATALYSIS

AHMAD LUQMANN BIN AFANDI

A thesis submitted in fulfillment of the requirements
for the award of the degree of
Bachelor of Engineering Technology (Energy & Environment) with Honors.

Faculty of Civil Engineering Technology
UNIVERSITI MALAYSIA PAHANG

FEBRUARY 2022

ACKNOWLEDGEMENTS

Firstly, all praises for the creator of the whole universe, almighty ALLAH, who from his countless blessings gave me the patience and wisdom to face the challenging task of this degree. we would like to acknowledge our great debt of gratitude to all, who helped us over this research period. we would like to express many thanks to our supervisor Assoc. Prof. Dr. Azrina Binti Abd Aziz for all kinds of mentoring, instructions, research writing, mock presentation, and support towards us enormously throughout our Degree studies. we are glad to have this opportunity to be students under her supervision because it was a great chance for learning knowledge and vast experience. We appreciate Dr. Azrina Binti Abd Aziz so much for her effort and continuous guidance in leading our team to achieve success in development on how to run this project and her constant encouragement and moral support to maintain our progress in the correct work.

We would like to use this opportunity to express our sincere thanks to our deepest appreciation to all those who provide us the possibility and gave us kind of assistance in accomplishing the project report regarding the “Scaling Up Anodic TiO₂ Nanotube Layers For Gas-Phase Photocatalysis”. Without valuable guidance, contribution, and assistance in the preparation and the completion of this study from these individuals, this project would not have been possibly seen the light of the day.

Especially, we would also like to address our limited thanks to our family for their unconditional support, both financially and emotionally throughout our Senior Design Project in designing and developing this project. Endless gratitude to our family for advice and guidance at the right time and for being a source of motivation in accomplishing this Senior Design Project. In addition, they have always been for us and we are thankful for everything they have helped us achieve. Last but not least, we are thankful and indebted to all those who helped me directly or indirectly completion of this project and research writing of the “Scaling Up Anodic TiO₂ Nanotube Layers for Gas-Phase Photocatalysis”

ABSTRAK

Carbon dioxide (CO₂) emissions are defined as releasing greenhouse gases and their precursors into the atmosphere over a defined area and period that harm living things at the surface. One of the best ways to solve the CO₂ problem is to use solar energy to photocatalytically convert CO₂ to hydrocarbons, generating renewable energy and photocatalytic CO₂ reduction using either artificial light or sunlight and demonstrating the fundamental mechanism of CO₂ photoreduction. Photocatalytic reactions on TiO₂ have lately seen a massive rebirth due to several novel tactics and discoveries that promise to dramatically boost the efficiency and specificity of such reactions by changing the titania scaffold and chemistry. Anodization, sol-gel, hydrothermal method, sonoelectrochemical, microwave irradiation, and alkaline synthesis are among the methods available for the production of TiO₂ Nanotubes. Among these methods, anodization is chosen. This research aims to design and fabricate the anodization reactor for TiO₂ nanotubes layers for gas-phase photocatalysis. Electrochemical anodization is the most widely used method because of its controllable, repeatable results in a single process, the ability to tune the size and shape of nanotubular arrays to the desired dimensions, and the ability to meet the demands of specific applications through controlled anodic oxidation of the metal substrate. It is also a cost-effective method, and the tubes created this way have good adherent strength. Furthermore, anodization parameters can easily control the thickness and morphology of TiO₂ films. The electrochemical anodization method was used as the anodization process to make the TiO₂ nanotubes. The material and the design were carefully chosen to make the anodization perfect. The amount of TiO₂ that can be produced can be increased by scaling up the anodization process. Several tests will be run to prove that the anodization scaling up was a success. The test used was Field Emission Scanning Electron Microscopy (FESEM), Energy Dispersive X-Ray Spectroscopy (EDX), and Cryogenic Transmission Electron Microscopy (Cryo-TEM). The use of CO₂ as a fuel in ovens, houses, and trucks highlights the benefits of converting to CH₄, which may even be used to generate energy. The consequent slew of global environmental issues poses a significant threat to human survival and the planet. As a result, it is a substantial obstacle to humanity's ability to lessen its reliance on fossil fuels and convert CO₂ into added-value chemicals and fuels.

ABSTRACT

Carbon dioxide (CO₂) emissions are defined as releasing greenhouse gases and their precursors into the atmosphere over a defined area and period that harm living things at the surface. One of the best ways to solve the CO₂ problem is to use solar energy to photocatalytically convert CO₂ to hydrocarbons, generating renewable energy and photocatalytic CO₂ reduction using either artificial light or sunlight and demonstrating the fundamental mechanism of CO₂ photoreduction. Photocatalytic reactions on TiO₂ have lately seen a massive rebirth due to several novel tactics and discoveries that promise to dramatically boost the efficiency and specificity of such reactions by changing the titania scaffold and chemistry. Anodization, sol-gel, hydrothermal method, sonoelectrochemical, microwave irradiation, and alkaline synthesis are among the methods available for the production of TiO₂ Nanotubes. Among these methods, anodization is chosen. This research aims to design and fabricate the anodization reactor for TiO₂ nanotubes layers for gas-phase photocatalysis. Electrochemical anodization is the most widely used method because of its controllable, repeatable results in a single process, the ability to tune the size and shape of nanotubular arrays to the desired dimensions, and the ability to meet the demands of specific applications through controlled anodic oxidation of the metal substrate. It is also a cost-effective method, and the tubes created this way have good adherent strength. Furthermore, anodization parameters can easily control the thickness and morphology of TiO₂ films. The electrochemical anodization method was used as the anodization process to make the TiO₂ nanotubes. The material and the design were carefully chosen to make the anodization perfect. The amount of TiO₂ that can be produced can be increased by scaling up the anodization process. Several tests will be run to prove that the anodization scaling up was a success. The test used was Field Emission Scanning Electron Microscopy (FESEM), Energy Dispersive X-Ray Spectroscopy (EDX), and Cryogenic Transmission Electron Microscopy (Cryo-TEM). The use of CO₂ as a fuel in ovens, houses, and trucks highlights the benefits of converting to CH₄, which may even be used to generate energy. The consequent slew of global environmental issues poses a significant threat to human survival and the planet. As a result, it is a substantial obstacle to humanity's ability to lessen its reliance on fossil fuels and convert CO₂ into added-value chemicals and fuels.

TABLE OF CONTENT

DECLARATION	
TITLE PAGE	
ACKNOWLEDGEMENTS	ii
ABSTRAK	iii
ABSTRACT	iv
TABLE OF CONTENT	v
LIST OF TABLES	viii
LIST OF FIGURES	ix
LIST OF SYMBOLS	x
LIST OF ABBREVIATIONS	xi
LIST OF APPENDICES	xii
CHAPTER 1 INTRODUCTION	1
1.1 Research Background	1
1.2 Problem Statement	6
1.3 Research Objectives	7
1.4 Scope of Research	7
1.5 Significance of Research	9
1.6 Outline of Thesis	10
CHAPTER 2 STYLES	11
2.1 Energy Demand and Environmental Impact	11
2.2 Climate Change and CO ₂ potential greenhouse gas	12
2.3 Fundamentals of Photocatalysis for CO ₂ Reduction	13
2.3.1 Principle of Photocatalysis for CO ₂ Conversion	14
2.3.2 Thermodynamics of Photocatalysis for CO ₂ Reduction	15

2.3.3	Mechanism of Photocatalysis Conversion/Reduction of CO ₂	16
2.4	TiO ₂ Based photocatalytic for CO ₂ conversion	18
2.4.1	TiO ₂ as photocatalyst	19
2.4.2	Amplifications in TiO ₂ -Based Photocatalytic CO ₂ Conversion	19
2.5	Advanced in TiO ₂ -based Nanocomposite Visible Light Photocatalyst (VLP)	23
2.6	Method of Synthesization (TNAs)	28
2.6.1	Hydrothermal	28
2.6.2	Electrochemical Anodization	29
2.6.3	Effects of Fabrication Factors on TNAs	30
2.7	Application of TNAs	35
2.7.1	Photocatalyst	35
2.7.2	Solar Cells	38
2.7.3	Water Splitting	39
2.7.4	Other Applications	41
2.8	Summary of Literature Review	42
 CHAPTER 3 METHODOLOGY		 44
3.1	Flowchart of Methodology	44
3.2	Design of Anodization Device	45
3.3	Consumables Selection	45
3.4	Manufacturing of Anodization Device	46
3.5	Proof Concept	48
3.5.1	Field Emission Scanning Electron Microscopy (FESEM)	48
3.5.2	Energy Dispersive X-Ray Spectroscopy (EDX)	49
3.5.3	Cryogenic Transmission Electron Microscopy (Cryo-TEM)	49

CHAPTER 4 RESULTS AND DISCUSSION	50
4.1 The Differences between the Lab Scale and The Up-Scale of The Reactor Design	50
4.2 The Selection for Fabricate Factors of Effects	51
4.2.1 Working Electrode Anode	51
4.2.2 Counter Electrode Cathode	51
4.2.3 Electrolyte	52
4.2.4 Voltage Apply	53
4.2.5 Anodization Time	53
4.2.6 Temperature	53
4.3 Schematic Diagram for Up Scale Reactor	54
CHAPTER 5 CONCLUSION	56
5.1 Conclusion	56
5.2 Recommendation	56
REFERENCES	57
APPENDICES	65

LIST OF TABLES

Table 2.1	Literature summary of TiO ₂ -based photocatalyst for the photocatalytic reduction of CO ₂	21
Table 2.2	Noble metal enhanced TiO ₂ -based photocatalyst for photocatalytic CO ₂ reduction.	25
Table 2.3	Summaries of various synthesis generations of TNA's	31
Table 2.4	Bandgap energies of semiconductors as photocatalyst.	36
Table 2.5	Summary of TNA-based materials in water splitting	40

LIST OF FIGURES

Figure 1.1	Mechanism for photocatalytic conversion of CO ₂ and CH ₄ by CuPc/TiO ₂ photocatalyst.	5
Figure 2.1	Thermodynamics and Gibbs free energy of photocatalyst under light and without light.	16
Figure 2.2	Narrowing and expansion of bandgap of the semiconductor.	16
Figure 2.3	Schematic illustration of photocatalytic CO ₂ reduction mechanism utilizing TiO ₂ semiconductor photocatalysts surface with elaborate reaction pathways.	17
Figure 3.1	Flowchart	44
Figure 3.2	Proposed design with dimension.	46
Figure 3.3	Proposed design for upscale anodization device.	47
Figure 3.4	The schematic diagram of an up-scale anodization device.	47
Figure 4.1	Up-scale schematic diagram	54
Figure 4.2	Electrode rack design	55
Figure 4.3	Reactor tank design	55

LIST OF SYMBOLS

%	Percent
°C	Celsius
°F	Fahrenheit
atm	Unit of pressure
cm	Centimeter
cm ²	Square centimeters
cm ³	centimeter
eV	Electronvolt
g/L	Gram per little
h	Hour
kJ mol ⁻¹	Kilojoule per mol
mA	Milliamperes
min	Minutes
mm	Millimeter
nm	Nanometer
ppm	Parts per million
V	Volt
μm	Micrometer

LIST OF ABBREVIATIONS

CB	Conduction band
CH ₄	Methane
CO ₂	Carbon dioxide
Cryo-TEM	Cryogenic Transmission Electron Microscopy
DSSCs	Dye-Sensitized Solar Cells
EDX	Energy Dispersive X-Ray Spectroscopy
FESEM	Field Emission Scanning Electron Microscopy
GHGs	Greenhouse gases
GWP	The Global Warming Potential
HF	Hydrofluoric acid
IPCC	Intergovernmental Panel on Climate Change
LOD	Detection limit
MCPA	Methylphenoxyacetic
NOMs	Natural organic matter
PAD	Polymer-assisted deposition
PCC	Photocatalytic CO ₂ conversion
PCCR	Photocatalytic CO ₂ reduction
QDSSCs	Quantum Dots Sensitized Solar Cells
RBA	Rapid breakdown anodization
RSD	Relative standard deviation
SDME	Single-drop microextraction
Ti	Titanium
TiO ₂	Titanium oxide
TNA	Titanium nanotube array
TNTs	Titanium oxide nanotubes
UNFCCC	United Nations Framework Convention on Climate Change
UV	Ultraviolet light
VB	Valence band
VLP	Visible Light Photocatalyst
IV	Instrumental variable

LIST OF APPENDICES

CHAPTER 1

INTRODUCTION

1.1 Research Background

The term "global warming" refers to the observed century-scale rise in the average temperature of the Earth's climate system, as well as its consequences. Scientists are almost certain that rising concentrations of greenhouse gases (GHGs) and other human-caused pollutants are to blame for virtually all of global warming. Accumulating such as water vapor, carbon dioxide, methane, nitrous oxide, and ozone capture and release heat radiation in the earth's atmosphere (Powell, 2019). Increasing or decreasing the amount of (GHGs) in the atmosphere allows the sun's heat to be kept in or released. Scientists agree that the earth's rising temperatures are fuelling longer and hotter heat waves, more frequent droughts, heavier rainfall, and more powerful hurricanes. For example, scientists confirmed in 2015 that global warming had exacerbated an ongoing drought in California (the state's worst water shortage in 1,200 years). They also claimed that the probability of potential droughts had approximately doubled over the previous century. In 2016, the National Academies of Science, Engineering, and Medicine announced that weather phenomena, such as heatwaves, can now be related to climate change with confidence (Amanda MacMillan Jeff Turrentine, 2021).

Carbon dioxide (CO₂) is a significant heat-trapping GHG that is released by human activities like deforestation and fossil fuel combustion, as well as natural processes like respiration and volcanic eruptions. Human activities have increased CO₂ concentrations in the atmosphere by 48% since 1850, compared to pre-industrial levels. This is significantly more than what would have occurred naturally over 20,000 years (from the Last Glacial Maximum to 1850, from 185 ppm to 280 ppm) (Holly Shaftel, Randal Jackson, Susan Callery & Daniel Bailey, 2021). While much of the media and public focus has been on the effects of higher CO₂ concentrations on global climate, rising CO₂ concentrations are also likely to have profound direct effects on plant growth,

physiology, and chemistry, independent of any effects on climate (Liu, 2017). The central importance of CO₂ in plant metabolism causes these effects. Plants absorb atmospheric CO₂ as photosynthetic organisms, reducing carbon in the atmosphere chemically. This not only provides the plant with stored chemical energy but also the carbon skeletons for the organic molecules that make up the plant's structure.

Businesses, factories, and other commercial facilities are responsible for a large portion of this increase. More heat is "trapped" in the earth's atmosphere as levels of (CO₂) and another GHG rise, causing global temperatures to rise. The amount and frequency of precipitation, as well as the timing and length of the seasons, are all affected. Rising sea levels, ecosystem changes, food insecurity, and an increase in extreme weather conditions such as flooding, droughts, hurricanes, and wildfires are all signs of climate change. (the University of Michigan. 2020) The industry sector produces goods and raw materials for everyday use, every single day. The GHG that industrial production emits is split into two categories. Direct emissions are GHG produced at the facility itself and indirect emissions are associated with the facility's use of energy but happen off-site. Energy used in factories and other facilities to run machines, process raw materials, run computers, connect to the internet, heat and cool buildings, and more can all contribute to carbon dioxide emissions. Leaks in the industrial process, chemical reactions during the manufacturing process, and the use of petroleum in production can all result in direct emissions. Indirect emissions are caused by energy production off-site, such as emissions from power plants that supply electricity to facilities. There are several ways to reduce CO₂ emissions and save the world. One of them is reducing reliance on fossil fuels. Coal combustion produces CO₂ emissions, which contribute to irreversible climate change. Businesses that make a conscious effort to switch to sustainable energy sources like wind or solar power can help to reduce CO₂ emissions daily (EPA, 2020). Carbon capture and storage is the traditional method for solving this problem, but it has never been completely solved because CO₂ does not convert into other substances (H. Yoneyama, 1997). The photocatalytic conversion of CO₂ to hydrocarbon fuels was discovered to be a promising method (Chao Peng, 2017). Due to its excellent stability, nontoxicity, and low cost, TiO₂ is one of the most promising semiconductor materials used in photocatalysis (A. Fujishima & K. Honda, 1972).

Photocatalysis is the activity occurring when a light source interacts with the surface of semiconductor materials, the so-called photocatalysts. At least two simultaneous reactions, oxidation from photogenerated holes and reduction from photogenerated electrons, must occur during this process. Because the photocatalyst should not change, the two processes must be precisely synchronized. In 1972, Fujishima and Honda's TiO_2 was later discovered to aid in the decomposition of cyanide in water, piquing interest in the material's environmental applications. TiO_2 is ideal for photocatalysis for a variety of reasons, including its widespread availability, low cost, and chemical stability. Photocatalysis can be used to decompose pollutants and improve the quality of the atmosphere's air in a real-world setting. As a result, photocatalysis can be used in the construction industry to improve indoor air quality (Papadaki, 2017). A photocatalyst converts solar energy into chemical energy, which can be used for environmental and energy applications like water treatment, air purification, self-cleaning surfaces, hydrogen production via water cleavage, and CO_2 conversion to hydrocarbon fuels. In the last two decades, there has been significant progress in the development of efficient photocatalytic materials, with a large number of research papers published each year. Advances in nanotechnology have largely correlated with improvements in the performance of photocatalytic materials (Rengui & Can, 2017).

Titanium dioxide (TiO_2) has been extensively researched for photocatalysis due to its many advantages, including high photocatalytic activity, excellent physical and chemical stability, low cost, non-corrosive, non-toxicity, and high availability. TiO_2 's photocatalytic activity is dependent on its phase. It comes in three different crystalline forms: anatase, rutile, and brookite. The metastable anatase phase has a higher photocatalytic activity than the rutile phase, which is more chemically stable but less active. When compared to pure anatase and rutile phases, some TiO_2 with a mixture of both anatase and rutile phases have higher activities. When TiO_2 is exposed to high-energy light, electrons from the valence band are promoted to the conduction band, leaving a hole, h^+ , in the valence band and an excess of negative charge in the conduction band. Both the free electrons in the conduction band and the resulting holes in the valence band are strong oxidizing agents and can participate in redox reactions. TiO_2 , on the other hand, has several drawbacks that limit its use in photocatalysis. To begin with,

photogenerated electrons and holes coexist in the TiO₂ particle, with a high likelihood of recombination. As a result, the desired chemical transformations occur at low rates about the absorbed light energy. Because of the relatively large bandgap energy (3.2 eV), photoactivation requires ultraviolet light, resulting in very low efficiency in utilizing solar light. When compared to visible light, UV light makes up only about 5% of the solar spectrum (45%). Furthermore, due to its non-porous nature and polar surface, TiO₂ has a low absorption capacity for non-polar organic pollutants. The recovery of nano-sized Titania particles from treated water is also a challenge, both economically and in terms of safety. Agglomeration and aggregation affect the photoactivity and light absorption of TiO₂ nanoparticles (John Moma, Jeffrey Baloyi, 2018).

Global scientists and researchers are working on developments in renewable energy such as wind, hydel, biomass, nuclear, and solar energy. Among these, solar energy, in terms of its utilization in converting anthropogenic CO₂ into value-added chemicals on a photocatalyst surface in the presence of a reducing agent, is an alluring and auspicious research area to counter environmental pollution with the possibility of matching the renewable energy infrastructure. CO, CH₄, C₂H₆, C₂H₅OH, C₂H₄, CH₃OH, HCOOH, and other value-added chemicals are produced by photocatalytic CO₂ conversion (PCC), in general mimics the concept of natural photosynthesis and are considered a subordinate of the “Artificial Photosynthesis” research domain. TiO₂ photocatalysts have emerged as the premier and champion material with superb properties such as favorable surface area, non-toxicity, abundant availability, high stability, and cost-effectiveness since the invention of water photocatalysis by Fujishima and Honda in 1972. On the other hand, TiO₂ nanoparticles (0-D) have fast electron-hole recombination, slow charge transfer, limited light trapping, and difficulty in reuse/recycling, in addition to the disadvantage of UV light absorption. Despite the development of many alternative photocatalysts to TiO₂, TiO₂ remains a prominent and preferred choice due to the specific characteristics listed above.

The suggested reaction mechanisms have been illustrated in Figure 1.1 for the photocatalytic synthesis of formate and acetate derivatives over CuPc/ TiO₂ photocatalyst from a gaseous mixture of CH₄ and CO₂. When the CuPc/TiO₂ film is exposed to visible light, the CuPc is first excited, resulting in the generation of an electron (e) in the CuPc

excited single state and a hole (h^+) in the CuPc ground state. The electron is then injected into TiO_2 's conduction band, where it undergoes a series of oxidation-reduction reactions. TiO_2 dye sensitization does extend light absorption into the visible spectral region. This is one of the main reasons why the CuPc/ TiO_2 photocatalyst film is more efficient when exposed to sunlight.

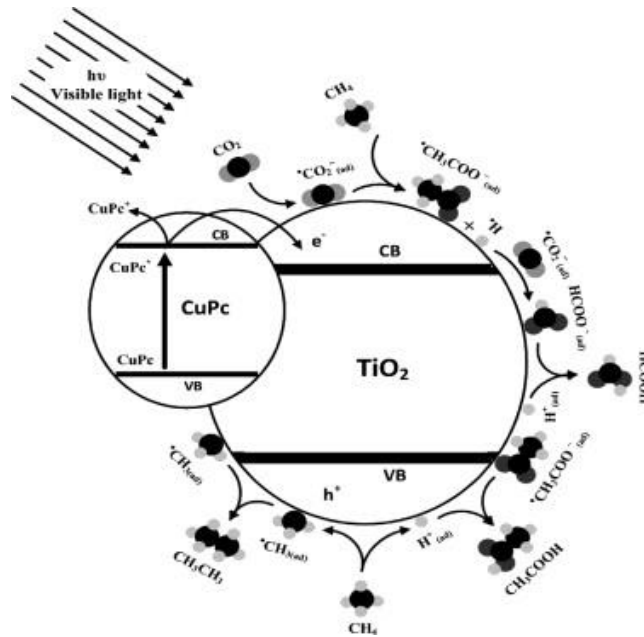


Figure 1.1 Mechanism for photocatalytic conversion of CO_2 and CH_4 by CuPc/ TiO_2 photocatalyst.

Source: (Shahram Sharifnia & Yazdanpour Neda, 2013).

Following the generation of electrons and holes, radical $\bullet\text{CH}_3$ is formed by oxidizing CH_4 with valence band holes, and H^+ is released at the same time. After that, two radical $\bullet\text{CH}_3$ may couple to form ethane. Furthermore, electrons in the conduction band reduce CO_2 to radical $\bullet\text{CO}_2$ radicals. Acetate is formed when the radical $\bullet\text{CO}_2$ is attacked by CH_4 (D. Shi, 2004). Acetic acid is formed when acetate reacts with H^+ . Formate is formed when radical $\bullet\text{CO}_2$ is attacked by radicals. H^+ and the formate produced reacts with H^+ to produce formic acid. Both reactants (CO_2 and CH_4) should be adsorbed on the illuminated TiO_2 surface in this photocatalytic reaction. The conversion of CH_4 and CO_2 to photocatalytic products is inhibited by increasing the concentration of radical $\bullet\text{CH}_3(\text{ad})$ and radical $\bullet\text{CO}_2^-(\text{ad})$ radicals and backward reactions. (Neda Yazdanpour, 2013).

1.2 Problem Statement

The high level of CO₂ emissions necessitates research into methods for converting CO₂ to CH₄. CO₂ pollution is harmful to our wellbeing and can threaten human existence if exposed for a prolonged period. CO₂ emissions are generated by several causes, like cars, mills, among others. If CO₂ emissions continue unchecked, they will claim numerous lives. Using evidence from a wide panel of countries from 1960 to 2017, the instrumental variable (IV) regression findings show that a 10% rise in per capita CO₂ pollution results in a 2.2 percent increase in crude mortality rate and a 0.6 percent decrease in life expectancy (Hailemariam, 2019). There is already convincing evidence that long-term exposure to CO₂ concentrations predicted by the end of the century will have a profound effect on humans. Unhealthy blood CO₂ concentrations have been measured in individuals in typical indoor environments, where concentrations of CO₂ greater than 600 parts per million have been found to affect thinking skills and induce health problems after relatively brief exposures. (Bierwirth, 2021). The method of converting CO₂ to CH₄ is already created by using photocatalysis.

Photocatalysis is a type of artificial photosynthesis that employs environmentally friendly, sustainable chemistry to address energy and environmental concerns (Dhinasekaran, Rakkesh, Saravanan R, & Mu. Naushad, 2020). Among these techniques is the photocatalytic removal of CH₄ and CO₂ to high-value materials, which is also the subject of this research. The following are the main problems discussed in this study:

- i. Due to the two-step conversion of CO₂ and CH₄ into hydrocarbon fuels, the reaction between CH₄ and CO₂ is uphill. This method needs further energy supply, which increases greenhouse gas pollution and results in uneconomical and environmentally damaging practices.
- ii. Conversion of CO₂ and CH₄ concurrently is known as a perfect redox reaction (KHANI, 2017).
- iii. Only manage to convert CO₂ to hydrocarbon fuel but in low amounts.

Due to its high photoactivity, high durability, low expense, and protection for the atmosphere and people, TiO₂ has been commonly used as a photocatalyst in several environmental and energy applications. However, due to its wide bandgap energy, it can consume only ultraviolet radiation, which accounts for approximately 5% of the solar spectrum. Additionally, the photocatalytic operation of TiO₂ is restricted by the photogenerated electron-hole pairs' rapid recombination (John Moma, Jeffrey Baloyi, 2018). Additionally, TiO₂ has a sluggish reaction pace, weak selectivity, and an inefficient reactor configuration, resulting in a low product yield. Additionally, TiO₂ is the most affordable, readily usable, and well-characterized UV light active semiconductor photocatalyst. TiO₂ exhibits low visible light absorption, accounting for 53% of the solar spectrum, resulting in an inadequate yield of solar product. Finally, the process of photocatalytic CO₂ conversion is called complex.

CO₂ emissions may be minimized by the conversion of CO₂ to CH₄. This method has already been effective in transforming it, but the issue is that the size of development of TiO₂ nanotubes was restricted to a few samples per experiment cycle. Increased development of TiO₂ Nanotubes (TNTs) would mean that far more CO₂ could be converted to CH₄ through gas-phase photocatalysis. The design and construction of the TiO₂ nanotube reactor will be discussed in this thesis.

1.3 Research Objectives

- i. To design up-scale TiO₂ anodization reactor or TNTs layers for gas-phase photocatalysis.
- ii. To produce TNTs by using the fabricated reactor.
- iii. To analyze the synthesized TiO₂ Nanotubes by using FESEM, Cryo-TEM, and EDX.

1.4 Scope of Research

This study focuses on how to create design and scale up the design of anodic TiO₂ nanotube layers for gas-phase photocatalysis. The photocatalytic activity is based on the formation of electron-hole pairs with sufficient energy to form radicals with high

oxidizing power (under UV light illumination). However, a large active surface area of the photocatalyst is also necessary for effective photocatalysis. As a result, in recent years, the use of nanostructured TiO₂, such as nanoparticles, nanorods, and nanotubes, prepared by various methods, has gotten a lot of attention. Many studies have shown that self-organized TiO₂ nanotube layers can be used to photocatalyze the degradation of pollutants. Anodization of Ti in a fluoride-containing electrolyte is a simple way to make these layers. The dimensions of nanotubes can be altered by altering the anodization parameters (electrolyte, anodization potential, anodization time). The fact that they adhere strongly to the underlying Ti substrate is their main advantage.

Most publications have only reported photocatalytic tests on a laboratory scale, for example using active catalyst areas of a few cm² more or less. This is due to the difficulty of controlling anodization process parameters on a larger scale. The main issue is the massive current that is received during the anodization of large substrates. As a result, the electrolyte temperature rises, potentially causing the dielectric breakdown of the growing nanotube layers. This undesirable event can be avoided by effectively cooling the electrolyte during the anodization process. However, there are only a few reports that show large-scale Ti substrates being anodized. These large-scale TiO₂ nanotube layers have only been used in the aqueous phase for photocatalytic degradation of various pollutants. (Hanna Sopha, *et al.*, 2018).

While designing the new anodization device, the design rationales of the device setup were initially evaluated, followed by proof of concept data, leading to further upscale and optimization. Design rationales include creating a scalable device design that was suitable for multiple specimens per batch of the anodization process and maintaining constant electrode distances for process control while ensuring device setup that was compatible with the use of hydrofluoric acid (HF). Also, there are several characteristics for design rationales which are even distribution of potential and current to all specimens, monitoring the potential of the working electrode during the anodization process, and no contamination from copper parts, which deleteriously affects the anodizing process and *in vitro* cell and tissue culture tests. Comparatively, design rationales include a counter electrode that was at least similar or larger area to that of the working electrode.

1.5 Significance of Research

The photocatalytic conversion of CO₂ to CH₄ using a synthesized nanocomposite photocatalyst is critical for the production of hydrocarbon fuel and reduction of the influential CO₂ greenhouse gas. These photocatalysts based on TNTs have been used in a limited number of applications for photocatalytic CO₂ reduction (KHATUN, 2020). Consumption of the greenhouse gas CO₂ through the process is an additional environmental advantage of the power to biomethane technology. Although the addition of an organic substrate can revitalize the entire biogas microbial community by increasing CO₂ production and thus stabilizing the pH, it does not promote the conversion of H₂ to CH₄. A correctly planned feeding routine results in a sustained high rate of CH₄ creation, enabling the machine to function effectively over a prolonged period. (Márk Szuhaj, dll., 2016). The usage of fuel for ovens, houses, and trucks demonstrates the advantage of switching CO₂ to CH₄ and can even be used to generate electricity. The resulting amount of global environmental problems pose a considerable challenge to human existence and the earth. It is thus a serious barrier for mankind not only to reduce human dependence on fossil fuels but also to transform CO₂ into the added value of chemicals and fuels (Yi, dll., 2020).

Conventional anodization systems are usually limited for production of in vitro specimens by the following factors:

- i. anodizing is limited to a specific specimen rather than the entire surface, leading to material wastage;
- ii. trimming of specimens for in vitro studies causes specimen damage;
- iii. usually, only one specimen can be accommodated in the system, and high volume production is typically expensive in cost and time; and
- iv. consistency and reproducibility cannot be guaranteed from specimen to specimen due to small variations in the anodizing conditions. consistency and reproducibility cannot be guaranteed from specimen to specimen due to small variations in the anodizing conditions.

The limitations above highlight the need for a tailored anodization device design to produce fully anodized surfaces and to increase the productivity and repeatability of the anodization process. In the present work, we designed an optimized anodization setup to reduce fabrication costs and to maximize the efficiency rate of anodizing titanium discs, for the first time, with the following objectives:

- i. to anodize the entirety of specimen surfaces to reduce excessive material waste;
- ii. to increase the number of specimens per anodized batch;
- iii. to anodize batches of specimens with consistent results;
- iv. to anodize specimens of desired TiO₂ nanotube pore diameters;
- v. to customize the specimen shape for actual practical application, in our case, for in vitro biocompatibility tests.

1.6 Outline of Thesis

Chapter 1 introduction presents the key focus of the current study is the research history of environmental and energy issues. A notice on global change, greenhouse emissions, the improvement of CO₂, non-renewable energy fossil fuels, photocatalyst semiconductors, and TiO₂-based photocatalysts is presented. The shortcomings of these particular experiments were often seen and specific theories of the study were sculpted. The study goals, scale, and importance of this current study have also been described.

Chapter 2 literature review brief about the energy demand and environmental impact, climate change, and CO₂ potential greenhouse gas, fundamentals of photocatalysis for CO₂ reduction, amplification in TiO₂-based photocatalytic CO₂ conversion, recent progress of the anodization device for TNT layers, and literature review summary.

In chapter 3, the methodology of this research. Detailed parameters that need to be considered in designing the anodization reactor were discussed in this chapter.

CHAPTER 2

STYLES

2.1 Energy Demand and Environmental Impact

In the sense of green development, the energy market presents a special challenge because of its scale, scope, trajectory, and long-lived properties. The existing energy infrastructure depends heavily on fossil fuels, which in 2009 represented 84% of global greenhouse gas emissions. As a result of population and economic development, global energy demand is growing fast, particularly in the major developing countries, accounting for 90% of the energy demand growth by 2035. Around the same moment, almost 20% of the world's population lacks energy connectivity. In the way we create, distribute and use electricity, we need a big change (OECD GREEN GROWTH STUDIES, 2011). Since the start of the modern age, increasing amounts of gases have been emitted into the environment to absorb the heat, thus reducing the global mean temperature. A rise in temperatures by only a few degrees would contribute to global change that will lead to unforeseen ecological consequences of huge economic and social turbulence.

Global warming is of necessity the explanation why carbon dioxide (CO₂) use has to be avoided. Gases such as CO₂ migrate to the upper atmosphere (the troposphere), under which they serve as a sunlight display. They make rays in the sun but avoid the re-emergence of heat radiation, just like the glass greenhouse. The effect is that the greenhouse heats, in this situation the whole planet (Bilen, dll., 2007). Renewable electricity generated directly from biomass, wind, and hydroelectric energy can alleviate these problems but alone is not sufficient to meet energy needs. Researchers also attempted to mitigate CO₂ from the environment amounts. Among other topics, carbon capture and storage, CO₂ use, CO₂ reduction to chemical agents, and hydrocarbon fuels have considerable scientific relevance for researchers (Fatema, 2020).

2.2 Climate Change and CO₂ potential greenhouse gas

Climate change is defined as a change in the state of the climate that can be detected (for example, using statistical tests) by changes in the mean and/or variability of its properties over time, typically decades or longer. Climate change can be caused by natural internal processes or external forces such as solar cycle modulation, volcanic eruptions, and long-term anthropogenic changes in atmospheric composition or land use. It's worth noting the United Nations Framework Convention on Climate Change (UNFCCC). Climate change is defined as "a change in climate attributed directly or indirectly to human activity that alters the composition of the global atmosphere in addition to natural climate variability observed over comparable periods." As a result, the UNFCCC distinguishes between climate change caused by human activities altering atmospheric composition and climate variability caused by natural factors (Planton & Serge, 2013).

Environmental effects of global climate change have already been observed. Glaciers have shrunk, ice on rivers and lakes has broken up earlier, plant and animal ranges have shifted, and trees have begun to flower earlier. Loss of sea ice, accelerated sea-level rise, more intense heat waves are all effects that scientists predicted would occur as a result of global climate change in the past. Scientists are confident that global temperatures will continue to rise for decades to come, due in large part to greenhouse gas emissions caused by human activities. Over 1,300 scientists from the United States and other countries make up the Intergovernmental Panel on Climate Change (IPCC), which predicts a temperature rise of 2.5 to 10 degrees Fahrenheit over the next century. The extent of climate change effects on individual regions will vary over time and with the ability of various societal and environmental systems to mitigate or adapt to change, according to the IPCC. The IPCC predicts that increases in global mean temperature of less than 1.8 to 5.4 degrees Fahrenheit (1 to 3 degrees Celsius) above 1990 levels will produce beneficial impacts in some regions and harmful ones in others. Net annual costs will increase over time as global temperatures increase. "The range of published evidence indicates that the net damage costs of climate change are likely to be significant and to increase over time," the IPCC states (Holly Shaftel, Randal Jackson, Susan Callery & Daniel Bailey, 2021).

The Global Warming Potential (GWP) was created to allow comparisons of different gases' global warming effects. It is a measure of how much energy metric tons of gas emissions will absorb over a given period in comparison to 1 ton of CO₂ emissions. The greater the GWP, the more a given gas warms the Earth over time when compared to CO₂. The most common period for GWPs is 100 years. Analysts can add up emissions estimates for different gases using GWPs, and policymakers can compare emissions reduction opportunities across sectors and gases using GWPs. CO₂ has a GWP of 1, regardless of the period used because it is the gas used as a reference. CO₂ has a long life in the climate system: CO₂ emissions cause increases in CO₂ concentrations in the atmosphere that will last thousands of years. Over 100 years, methane (CH₄) is estimated to have a GWP of 28–36. Today's CH₄ emissions last about a decade on average, which is significantly less time than CO₂. However, CH₄ absorbs a lot more energy than CO₂. The GWP reflects the net effect of the shorter lifetime and higher energy absorption. The CH₄ GWP also considers some indirect effects, such as the fact that CH₄ is a precursor to ozone, which is a GHG in and of itself (EPA, 2020).

2.3 Fundamentals of Photocatalysis for CO₂ Reduction

In the presence of a catalyst, photocatalysis can be described as the acceleration of a photoreaction. In contrast with the metals that have an electrical spectrum, semiconductors resist energy area or bandgap, from the peak of the filled valence band (VB) to the base of the empty conduction band (CB) (Kočí, Obalová, & Lacný, 2007). Photocatalytic CO₂ reduction (PCCR) is one of the relevant research domains for "Artificial Photosynthesis" with a photocatalyst for converting CO₂ into the sunlight, in the presence of reducing agents such as H₂O, H₂, etc (CO, CH₄, CH₃OH, HCOOH, etc.). PCCR, therefore, can imitate natural photosynthesis because of its high performance and viability. PCCR provides two advantages:

- i. Clean energy fuel production that is adaptable to the existing energy grid; and
- ii. Standardization of anthropogenic CO₂ emissions while minimizing air emission and climate change (Ali, Adbul, & Su-Il, 2019).

Thermodynamically, CO₂ conversion is usually an endothermic method that involves a large input of energy and/or a high-energy reactor. The energy of C=O dissociation in CO₂ is ~750 kJ mol⁻¹, higher than many other chemical bonds such as C–H (~430 kJ mol⁻¹) and C–C (~336 kJ mol⁻¹). A strong activation barrier for CO₂ transformation can generally be resolved. The thermodynamic stability and kinetic inertness of CO₂ transform CO₂ in chemical sciences into a highly demanding research subject (Xie, Zhang, Liu, & Wang, 2016).

2.3.1 Principle of Photocatalysis for CO₂ Conversion

CO₂ is believed to be the strong and greatest driver to the global change of all greenhouse gases. Photocatalysis is a promising technology for addressing emerging global industrial CO₂ pollution concerns. Photocatalysis uses green solar power semiconductive content to reduce CO₂ to use a variety of high-value fuels such as methane, methanol, formaldehyde, and formic acid. Here, there is a brief discussion of the kinetic and thermodynamic concepts of CO₂ reduction and a description of the process and pathway for CO₂ reduction. Methods for improving CO₂ adsorption on the semiconductor surface are also discussed. The TiO₂ semiconductor is now commonly studied for its photocatalytic capacity to reduce CO₂ when properly modified due to its effective photoactivity, high stability, low costs, and protection. The latest TiO₂ synthesis and modification techniques that can be used to make the CO₂ photoreduction process more efficient are listed. These modification techniques, including metal deposition, metal/non-metal doping, carbon content charge, semiconductor heterostructure, and dispersal help, aim to increase the absorption of light, charge separation, and TiO₂ active surface, plus increase product yield and selectivity (Al Jitan, Palmisano, & Garlisi, 2020).

Photocatalytic transfer of CO₂ to renewable fuel using solar power has been deepened, both as this technique will reduce the level of greenhouse gas and alleviate the electricity shortfall. Although certain metal oxides (for example TiO₂ and WO₃) and non-oxides (for instance CdS and Ta₃N₅) are commonly used as photocatalysts, their photocatalytic reaction efficiency is still very poor. The construction of photocatalysts (typically type II heterojunctions) in hetero-structures is a common and efficient way of broadening the lighting area and improving the separation efficiency of photo-induced electron-hole pairs that eventually lead to better photocatalytic action. The redox

capability of photo-excited and hollow electrons in general type-II Heterojunction Systems is always weakened by the fact that the photo-generated electric in one semiconductor's CB will transfer from a relatively lower band-edge position to the CB of another semiconductor while the accumulated hole would transfer to the VB of the semiconductor with one hour (Yang, dll., 2019).

2.3.2 Thermodynamics of Photocatalysis for CO2 Reduction

The thermodynamics of photocatalysis can be discussed in terms of temperature, light, CB, and VB of semiconductors. Generally, a semiconductor may have filled VB and partially filled or empty CB. The forbidden energy level between VB and CB is called bandgap energy (E_g) and the energy levels of atoms have a different population of electrons (holes). When a semiconductor is exposed to light with energy $> E_g$, it disturbs the population of electrons and holes in CB and VB, respectively. Electrons are likely to achieve internal equilibrium within energy level rather than across bandgap because relaxation time within conduction band is shorter than across the bandgap as shown in Figure 2.1 and Figure 2.2. States of electrons with internal equilibrium are called quasi-equilibrium states and the potential of electrons and holes in quasi-fermi levels are given by Equations 2.1 and 2.2.

$$F_n = E_C + k_B T \ln \left(\frac{n}{N_C} \right) \quad 2.1$$

$$F_p = E_V + k_B T \ln \left(\frac{p}{N_V} \right) \quad 2.2$$

Where E_C and E_V are CB minimum and VB maximum energy level positions, k_B = Boltzmann constant, N_c and N_v are effective densities of states in CB and VB, n and p are carrier's concentration (Shehzad, Muhammad, Johari, Murugesan, & Hussain, 2018).

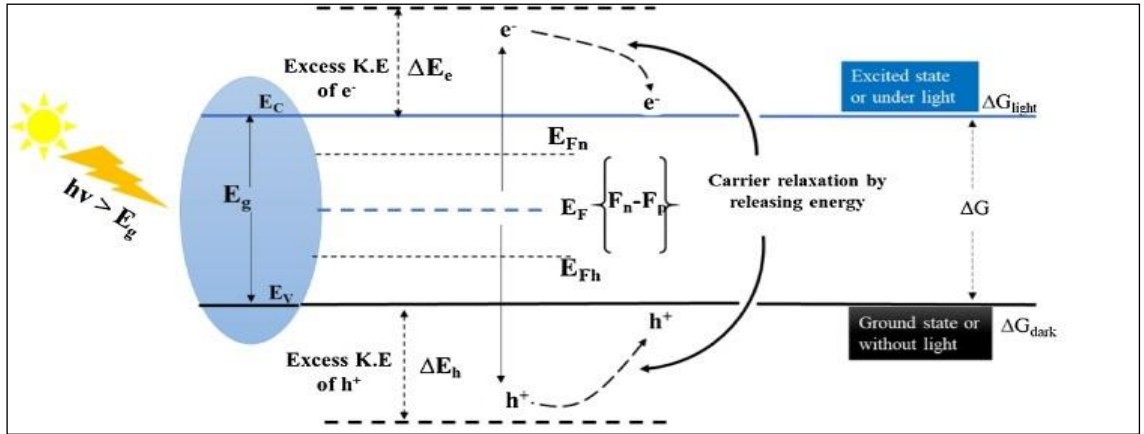


Figure 2.1 Thermodynamics and Gibbs free energy of photocatalyst under light and without light.

Source: (Shehzad, Muhammad, Johari, Murugesan, & Hussain, 2018).

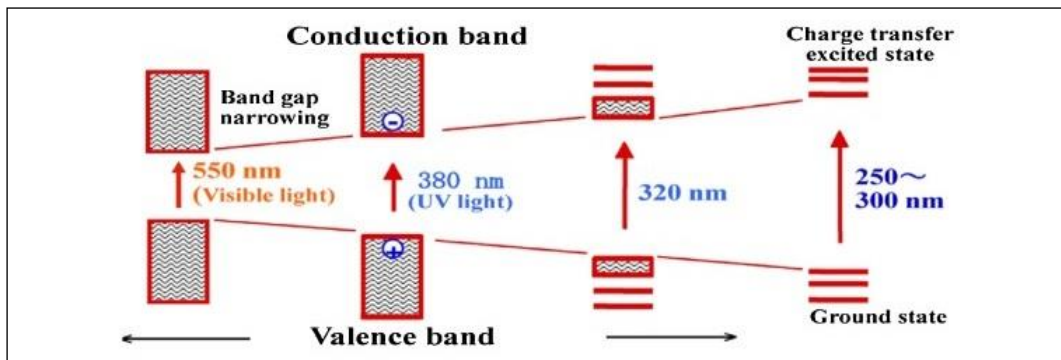


Figure 2.2 Narrowing and expansion of bandgap of the semiconductor.

Source: (Shehzad, Muhammad, Johari, Murugesan, & Hussain, 2018).

2.3.3 Mechanism of Photocatalysis Conversion/Reduction of CO₂

The photocatalytic mechanism for CO₂ reduction over a semi-conductor catalyst through suitable redox co-catalysts to shape solar fuels. The photocatalyst generates under excited conditions (light absorption) electrons that move from the VB to the CB, contributing to valence band holes. The migration to the catalyst's surface of the excited electron-hole pair initiates a CO₂ reaction to fuels and H₂O oxidization to O₂ (Li, Peng, & Peng, 2016).

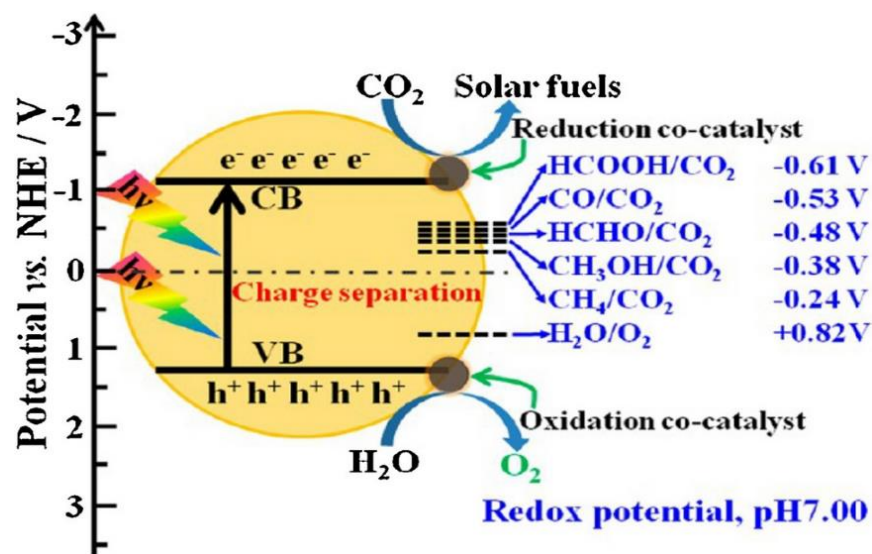
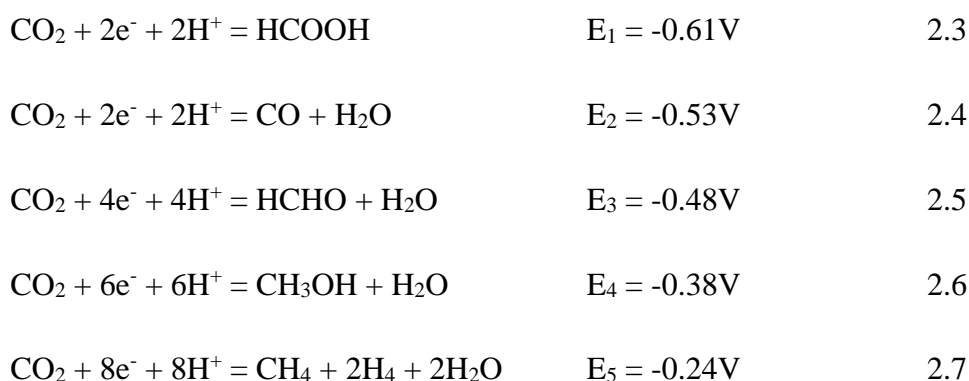


Figure 2.3 Schematic illustration of photocatalytic CO₂ reduction mechanism utilizing TiO₂ semiconductor photocatalysts surface with elaborate reaction pathways.

Source: (Li, Peng, & Peng, 2016).

A photocatalyst consumes light energy by electron photo excitation through the bandgaps and utilizes this energy to promote the chemical compound's surface reaction. It consists primarily of three key steps: light absorption, charge separation, and catalytic reaction on the surface. Photocatalysts produce electrons migrating from the valence band to the conduction band (light absorption) under some exciting conditions that lead to a hole in the valence band. The migration to the catalyst surface of the excited electron-hole pair starts the reduction in CO₂ reaction and oxidation of H₂O to O₂ (Khan & Muhammad, 2019). CO₂ is an extremely stable linear molecule with C=O bond energy at 298 kJ/mol, increasing the energy input required to reduce the CO₂ reaction. It is essential to use photocatalysts with the appropriate band structures that can be excited easily from the light source. Nevertheless, the one-electron reduction would not support CO₂ photocatalysis, because redox potential is strongly negative (-1.90 V vs. Standard Hydrogen Electrodes (NHE)) at pH 7.00. On the opposite, proton-assisted multi-electron reduction steps are commonly used as their lower redox potential (vs NHE at 7.00 pH) promotes CO₂-photocatalysis shown in Equations 2.3 until 2.7 (Kumar, *et al.*, 2019).



Generally speaking, the transition to the surface of adsorbed CO_2 species of photogenerated electrons for conversion into fuel is improved if the CB amount is significantly above the redox potential of the CO_2 and its reduced components (Ochedi, Liu, Yu, Hussain, & Liu, 2020).

2.4 TiO_2 Based photocatalytic for CO_2 conversion

Carbon dioxide capture, utilization, and storage (CCUS) including conversion to valuable chemicals is a complex contemporary problem with many facets. This review looks at the possibility of using CO_2 as a feedstock for synthetic applications in the chemical and fuel industries via carboxylation and reduction reactions. The current state of heterogeneously catalyzed hydrogenation, as well as photocatalytic and electrocatalytic activations of CO_2 to value-added chemicals, is discussed. Three stages of development are envisaged for CO_2 as a viable alternative to natural gas and oil as a carbon resource for the chemical supply chain:

- i. existing mature technologies (such as urea production);
- ii. emerging technologies (such as formic acid or other single carbon (C1) chemicals manufacture); and
- iii. innovative explorations (such as electrocatalytic ethylene production).

It has been identified and highlighted. The use of CO_2 which comes from existing petrochemical plants in reactions with commodity petrochemicals (such as methanol, ethylene, and ethylene oxide) produced at the same or nearby complex in order to

added products while also contributing to CO₂ fixation is a unique aspect of this review. It is estimated that ethylene oxide facilities around the world produce about 3 million tonnes of CO₂ per year. Such a CO₂ resource, which is already separated in pure form as part of the process, should be converted to a value-added chemical there, rather than being discharged into the atmosphere as is currently done. (Erdogan Alper, 2017)

2.4.1 TiO₂ as photocatalyst

The use of titanium dioxide as a photocatalyst has sparked a wide range of research studies and applications since Fujishima and Honda discovered the occurrence of water splitting on TiO₂ electrodes in 1972. Applications such as air and water purification, deodorization, antibacterial use, and self-cleaning are now possible. Because the bandgap of pure TiO₂ is large (3.2 eV), its photocatalytic property is active in the ultraviolet region, which accounts for about 10% of total solar intensity. The synthesis and application of TiO₂-based photocatalyst with enhanced visible light response are discussed in this presentation. The chemical solution technique, polymer-assisted deposition (PAD), was used to grow TiO₂ and C-doped TiO₂ films on ITO glass by heating Ti-polymer precursor films at temperatures ranging from 300 to 550 °C. SEM, XRD, and UV-V spectra are used to analyze the structure. The bandgap was found to be 3.05 eV at 500 °C, and it increased linearly with temperature as more of the polymer was burned off. The remaining polymer in TiO₂ annealed at 350 °C resulted in lower bandgap energy of 1.95 eV. TiO_{2-x}C_x has a reduced bandgap at temperatures below 400°C and should have visible light photocatalytic properties. The crystallinity of the C-doped TiO₂ films, on the other hand, is reduced to the point where the films become amorphous, resulting in no visible light activity. This finding is unique in that it demonstrates that lowering the bandgap energy can improve photocatalytic efficiency, but it does not guarantee it. (AIChE, 2010).

2.4.2 Amplifications in TiO₂-Based Photocatalytic CO₂ Conversion

At any time TiO₂ has become one of the most widely used photocatalysts in the energy and environmental domains since Fujishima and Honda (1972b) demonstrated water splitting on TiO₂ electrodes. Furthermore, TiO₂ has emerged as an ideal photocatalyst due to its diverse properties, such as nontoxicity, high photostability, and higher photoactivity. This semiconductor photocatalyst is widely used in a variety of

fields, such as biomedicine, wastewater treatment, and photocatalytic processes. (Neda Yazdanpour, 2013) Pure titanium dioxide has three common mineral phases: anatase, brookite, and rutile. The anatase and rutile phases of TiO_2 are the most studied for artificial photosynthesis of CO_2 (Chen et al., 2014). Chen et al. (2009) demonstrated that the anatase-dominated mixed phase has a higher visible light absorption capability and is more beneficial to CO_2 photoreduction. Yu, Low, Xiao, Zhou, and Jaroniec (2014) described a novel anatase TiO_2 for photocatalytic CO_2 reduction with co-exposed facets. In this study, CH_4 was discovered as a product. Yamashita et al. (1995) reported highly dispersed active titanium dioxide for photocatalytic reduction to CH_4 , CH_3OH , C2-compounds, CO , and O_2 under UV light irradiation. Table 2.1 shows a literature review of the TiO_2 -based photocatalytic CO_2 reduction approach, as well as some basic process parameters.

Table 2.1

Literature summary of TiO₂-based photocatalyst for the photocatalytic reduction of CO₂

TiO ₂ -based photocatalyst	Reductant	Catalyst synthesis method	Reaction condition	Photocatalytic reactor	Product yield	Light source	Reference
TiO ₂	H ₂ O	Commercial, P25 bar, 80 °C)	0.5 g/L, 7 bar, 80 °C	Pressurized batch reactor (20	H ₂ / HCHO/HCOOH 102/ vapor mmol/kg. h	125 W, medium- pressure vapour UV range (254 nm-364 nm)	(Galli et al., 2017a) Hg lamp,
MoS ₂ -TiO ₂	H ₂ O	Hydrothermal	50 mg sample with 100 mL H ₂ O, 25°C, 100kPa, 6h	Labsolar-6A The system, 500 cm ³ cylinder reactor	CO/ CH ₄ 268.97 μmol/g.cat/ 49.93 μmol/g.cat	300 W, Xenon arc lamp, visible light	(Jia et al., 2019)
1D-TiO ₂ nanotubes	H ₂ O	Hydrothermal	50 mg sample with 100 mL H ₂ O, 25°C, 101kPa, 600mL/min reactant (CO ₂ + H ₂ O) flowrate; 30 min/ 9h	Labsolar-6A system, 500 cm ³ cylinder reactor	CH ₄ / H ₂ 19.16 μmol/g.cat/ 12.71 μmol/g.cat	300 W, Xenon arc lamp, with UV 420 nm bandpass filter, visible light	(Huang et al., 2019)
TiO ₂ /Ti ₃ C ₂	H ₂ O	Simple calcination	50 mg sample with 100 mL H ₂ O, 80 °C, 6h	Pyrex reactor, 200 mL	CH ₄ 0.22 μmol h ⁻¹ C ₂ H ₅ OH, CH ₃ OH	300 W, solar simulated solar Xe arc lamp	(Low, Zhang, Tong, Shen, & Yu, 2018)
Reduced graphene oxide (rGO) wrapped	H ₂ O	Electrochemical anodization	15 mm × 20 mm × 0.25 mm (Ti plate size), 2 h	Cylindrical quartz reactor (50mm height,	CO / 760 μ Mol/g	200 W, UV-A lamp	(Rambabu et al., 2019)

Table 2 Continued

TiO ₂ -based photocatalyst	Reductant	Catalyst synthesis method	Reaction condition	Photocatalytic reactor	Product yield	Light source	Reference
-TiO ₂ nanotubes with multi-leg morphology (MLNTs)				20 mm inner diameter)			
Cu/TiO ₂ -SiO ₂	H ₂ O	One-pot sol-gel	25 °C, 1 atm, 100 and 3.0 mL/min reactant (CO ₂ + H ₂ O) flowrate	Stainless steel reactor, 6.0 cm × 2.5 cm	CO/ 60 μmol/g.cat .h CH ₄ / 10 μmol/g.cat .h	Xe arc source system, UV light (250 nm < λ 0 < 400 nm	(Li et al., 2010)
rGO-TiO ₂	H ₂ O	Solvothermal	Catalyst powder	Homemade continuous gas flow quartz reactor	CH ₄ / 0.135 μmolgcat ⁻¹ h ⁻¹	15 W, energy-saving daylight bulb, visible light	(Tan, Ong, Chai, & Mohamed, Homogene
Homogeneous ly hybrid TiO ₂ / ZnO mesoporous french fries (MousFFs)	H ₂ O	Furfural alcohol-derived polymerization -oxidation (FAPO)	0.1 g catalyst powder	Glass reactor (8.1 cm ²)	CH ₄ / 55 μmol g ⁻¹ h ⁻¹	300 W, Xe arc lamp	(Xi, Ouyang, & Ye, 2011)

2.5 Advanced in TiO₂-based Nanocomposite Visible Light Photocatalyst (VLP)

Semiconductor photocatalysis is recognized as a viable method for addressing both energy requirements and environmental degradation at the same time. Because of its low expense, nontoxicity, and high chemical stability, TiO₂ has been investigated for such applications. However, pristine TiO₂ also has a poor visible light consumption rate and a strong photogenerated charge-carrier recombination rate. TiO₂ photocatalysts changed by dual cocatalysts with different functions have recently received a lot of publicity because of the increased light absorption, improved reactant adsorption, and promoted charge carrier separation efficiency provided by various cocatalysts. The most recent advances in the part and structural design of dual cocatalysts in TiO₂ photocatalysts are summarised. Dual cocatalysts decorated on TiO₂ photocatalysts are classified into the following groups based on their components (Aiyun, Liuyang, Bei, & Jianguo, 2019):

- i. bimetallic cocatalysts;
- ii. metal-metal oxide/sulfide cocatalysts;
- iii. metal–graphene cocatalysts; and
- iv. metal oxide/sulfide–graphene cocatalysts.

Because of their strong photocatalytic activity, low expense, recyclability, and ability to oxidize and reduce most organic contaminants, TiO₂-based nanomaterials have been extensively researched and commonly used. TiO₂ produces hydroxyl (OH) radicals, which are more efficient than ozone and other AOPs used to degrade environmental contaminants. TiO₂ has poor photocatalytic performance in visible light, however, because its bandgap energy (3.0–3.2 eV) must be enabled by ultraviolet (UV) light, and solar light produces just 5% UV light. Furthermore, TiO₂ has a strong degree of recombination between the electron (e⁻) and hole (h⁺) pairs (Imran, Seu-Run, Sung-Pil, & Jong-Oh, 2017). To create VLP photocatalysts with improved photoactivity, selectivity, and solar light, an abundant and renewable resource could be used to convert CO₂ into value-added solar fuels and chemicals. Different noble metals (Pt, Au, Ag, Cu, and Pd) play a significant role after doping in TiO₂ in photocatalytic performances (Fatema, 2020).

Through the use of the absorption of visible light by metal nanoparticles, the usage of noble metals loaded on semiconductor supports has opened up new avenues for improving catalytic efficiency under light irradiation (Yu, dll., 2017). The surface plasmon resonance effect is caused primarily by the mutual oscillations of electrons on noble metal surfaces, and these energetic electrons pass into the coupled semiconductor's CB through the Schottky barrier. The Schottky barrier between noble metals and semiconductor oxides is created as a result of Fermi level equilibrium, and as a result, an electric field is formed at the interface that favors the separation of photogenerated charges (M. Humayun, F. Raiq, A. Khan, & W. Luo, 2018). Meanwhile, the photogenerated holes will remain on TiO_2 .

As a result, spatial isolation of photogenerated electron-hole pairs is possible. Furthermore, the working mechanism of metal is critical in deciding the electron-hole separation efficiency across the metal- TiO_2 interface. The metal's electron-accepting potential improves as the work activity of the metal increases, thus improving electron-hole isolation. Platinum has the highest work feature and the finest photocatalytic performances, and it is the most widely used co-catalyst with TiO_2 for photocatalytic CO_2 reduction. The improved photocatalytic efficiency of platinum-noble metal as a photocatalyst for CO_2 reduction to CH_4 . Another valuable property of noble metal-semiconductor nanocomposite is that it decreases the bandgap energy of the semiconductor, which slows photogenerated charge-carrier recombination. The bandgap energy of copper-modified TiO_2 was reduced from 3.2 eV to 2.34 eV, and the visible light reaction of the modified photocatalyst was extended up to 600 nm. They also discovered a 21-fold increase in CH_4 yield from photocatalytic CO_2 reduction with water by Cu deposited TiO_2 relative to commercial P_{25} TiO_2 (Jingxiang, Bei, & Jiaguo, 2017).

A summary of noble plasmonic metal enhanced based photocatalysts performance for the photocatalytic CO_2 reduction has been represented in Table below.

Table 2.2

Noble metal enhanced TiO₂-based photocatalyst for photocatalytic CO₂ reduction.

Noble metal-TiO ₂ photocatalyst	Reductant	Catalyst preparation method	Light source	Reactor	Yield enhancement	Remark
(Pt/TiO ₂) @ rGO	H ₂ O	Self-assembly method of simple and chemical reactions	Visible light (300 W xenon lamp, intensity 80 m Wcm ⁻²)	Gas-closed circulation system	CH ₄ /41.3 μmolg ⁻¹ h ⁻¹	The significant 31-fold enhancement of CH ₄ production obtained compared with commercial P ₂₅
Au-TiO ₂	H ₂ O	Deposition-precipitation	UV (6 W lamp, <365 nm, intensity, 71.7 Wm ⁻²) and 30 W white light LED, 400 and 455 nm)	Gas-phase homemade steel photoreactor with borosilicate window	CH ₄ / 8.0 μmolg _{cat} ⁻¹ h ⁻¹ (UV) CH ₄ , CO and H ₂ (visible light)	12 times higher CH ₄ production than TiO ₂ under UV irradiation, in the visible region the enhancement rate is not significant compared with TiO ₂ due to the excitation sub-bandgapgap electrons from surface defects
Pd-loaded TiO ₂ nanowires (Pd/TiO ₂ -NWs)	H ₂ O	Hydrothermal	Visible light (400 W Hg lamp)	Pyrex glass reactor containing cooling water	CH ₄ / 26.7 μmolg ⁻¹ , CO/ 50.4 μmolg ⁻¹	The CH ₄ production rate is higher than the TiO ₂ The CH ₄ production rate is higher than the TiO ₂ The CH ₄ production rate is higher than the TiO ₂
Pt-Ru nanocrystal	H ₂ O	Photon-assisted gas bubblingmembrane reduction (PGBMR)Photon-assisted gas bubblingmembrane reduction (PGBMR)	Visible light (300 W xenon lamp)	Watch-glass reactor with basal the basal diameter of 6.5 cm	CH ₄ / 38.7 μmolg ⁻¹ h ⁻¹ , CO/ 2.6 μmolg ⁻¹ h ⁻¹	The formation rate of CH ₄ (38.7 μmol g ⁻¹ h ⁻¹) is about 29-fold of commercial P ₂₅
Ag/TNTAs-E	H ₂ O	Photodeposition	Visible light (300 W, xenon arc lamp)	Pyrex reactor	CH ₄	The photocatalytic activity is higher than Ag/TNTAs-C and TNTs

Au Pd/3DOM- TiO ₂	H ₂ O	Gas bubblingassisted membrane reduction precipitation (GBMR)	Visible light, 300 W, xenon lamp)	Watch-glass reactor with basal the basal diameter of 6.5 cm	CH ₄ / 41.6 μmolg ⁻¹ h ⁻¹	The formation rate of CH ₄ over Au ₃ Pd ₁ /3DOM-TiO ₂ catalyst is about 11, 3, 1.8 times as high as that of 3DOM-TiO ₂ , Au ₄ /3DOMTiO ₂ , and Pd ₄ /3DOM-TiO ₂ catalysts, respectively
Au/Ag/TiO ₂ - NWs	H ₂	Chemical reduction and photodeposition	Visible light (35 W HID xenon lamp, intensity 20 mWcm ⁻²)	Stainless steel rectangular reactor, 108 cm ³	CH ₄ / 35 μmolg ⁻¹ h ⁻¹ , CO, C ₂ H ₄ , C ₂ H ₆ , C ₃ H ₆ , C ₃ H ₈ , CH ₃ OH	The yield rate of CH ₄ production was higher for Au/Ag/TiO ₂ NWs than TiO ₂

Source: (Fatema, 2020)

Noble-metal semiconductor-rich photocatalysts have shown outstanding photocatalytic efficiency in the reduction of CO₂ to hydrocarbon fuels and other chemicals. Although the cost of noble metals is high enough to render it a profitable photocatalyst for CO₂ reduction, its effectivity against light irradiation, as a dopant with semiconductor, enhanced commodity yield Table above could surpass all obstacles.

In different environmental applications, and environmentally safe photocatalytic process with TiO₂ as a photocatalyst has been used. The most researched applications include air, water, and wastewater treatment; inactivation of microorganisms such as bacteria and viruses; hydrogen generation by water splitting; dye-sensitized solar cells; and CO₂ processing into usable hydrocarbons. TiO₂ materials are used in many of these applications in a variety of morphologies, including zero-dimensional (nanoparticles), one-dimensional (wires, rods, and tubes), two-dimensional (layers and sheets), and three-dimensional structures (spheres). Because of the good combination of their peculiar physical properties with a well-controllable nanotubular structure, one-dimensional nanostructures, especially TNTs, have gained growing scientific attention. Their electronic properties, in particular, such as high electron mobility or quantum confinement effects, low dimensionality, and high surface-to-volume ratio, are of particular interest. As a result, the activity/reactivity of these systems increases dramatically. TNTs can be used as photocatalytic materials due to their unusual properties; however, their photoactivity is limited to the ultraviolet light region due to a wide bandgap (3.2 eV), which constitutes just 4% of total solar energy (P. M., dll., 2017).

Many studies, in particular, have been published on the use of self-organized TNTs layers for photocatalytic degradation of contaminants. Anodization of Titanium in a fluoride-containing electrolyte is a simple way to create these layers. The measurements of the nanotubes can be altered by adjusting the anodization parameters (electrolyte, anodization potential, anodization time). Their primary benefit is that they bind closely to the underlying Titanium substrate. This means that, unlike nanoparticles, no further immobilization is needed. Furthermore, because of the TNTs' vertical orientation on the Titanium substrate, increased charge separation is possible, which derives from the nanotubes' uni-directional dimensionality, resulting in better efficiency in photoelectrochemical applications. All of these properties are advantageous in photocatalysis, especially when an external potential is added (Hanna, dll., 2018).

TNTs photocatalytic activity was enhanced, allowing them to be widely used in power sources and low-power-consuming materials. The nano-hybrid architectures increase the system's working surface area and smartness. In the current study, TNTs arrays (TNAs) were created using a normal anodization technique, and the acetone sensing experiments were carried out in the presence of visible light in an in-house fabricated gas sensing chamber. By absorbing blue light emitted by commercially available LEDs, TNAs improve acetone sensitivity; we then investigated the photoinduced acetone sensing process. The experiments were carried out with differing concentrations of acetone vapors ranging from 10% to 50% in the absence and presence of the sun. It was discovered that at room temperature, the samples in the presence of visible light had a shorter corresponding duration and higher sensitivity than the samples in the absence of visible light (K. Ganesh, B.S., Mohammad, & Jihen, 2020).

2.6 Method of Synthesization (TNAs)

Anodization, sol-gel method, template method, hydrothermal method, sonoelectrochemical, microwave irradiation, and alkaline synthesis are among the methods available for the production of TNT. Hoyer was the first to report the template-assisted synthesis of TiO₂-based nanotubes. (Hoyer, 1996) TNT was then manufactured using electrochemical anodization and hydrothermal methods. Electrochemical anodization is the most widely used method because of its controllable, repeatable results in a single process, the ability to tune the size and shape of nanotubular arrays to the desired dimensions, and the ability to meet the demands of specific applications through controlled anodic oxidation of the metal substrate. It's also a cost-effective method, and the tubes created this way have good adherent strength. Furthermore, anodization parameters can easily control the thickness and morphology of TiO₂ films. (K. Indira, 2015).

2.6.1 Hydrothermal

Hydrothermal synthesis of TNAs was carried out using ammonium hexafluorotitanate as a deposition solution and anodic aluminum oxide attached to an aluminum substrate as a template. The as-prepared nanotube arrays were characterized using field emission scanning electron microscopy, energy-dispersive X-ray spectroscopy, and X-ray photoelectron spectroscopy, and the nanotube arrays' formation

mechanism was discussed. The findings show that the length of hydrothermal treatment has a significant impact on the formation of nanotube arrays with a homogeneous morphology, with 90 minutes being the optimum reaction time under the experimental conditions. This method produces TNAs with a unique morphology, which includes a continuous porous surface and discrete tubular cross-section structure. The preferential deposition of the hydrolysis product on the surface of the template, which is caused by the different reaction rate when $[\text{TiF}_6]_2$ reacts with the surface and the cross-section of the template, is attributed to the formation of such an especial morphology. (Gang Li, 2009).

2.6.2 Electrochemical Anodization

The electrochemical anodization of Ti thin foils in various electrolytes was used to create the second, third, and fourth generation of highly ordered titania nanotubular photoanodes. A scanning electron microscope analysis using a field emission gun revealed that films made up of nanotubes have a porous tubular morphology. The presence of anatase/rutile phase in annealed titania nanotubes was confirmed by X-ray diffraction results. The band-gap for various generation TNAs was 3.0, 2.8, and 2.5 eV, according to diffuse reflectance UV-Vis spectra analysis. When compared to their bulk counterparts, one-dimensional (1-D) highly ordered nanotube architectures with high surface-to-volume ratios have useful and unique properties. For vectorial charge transfer between interfaces, they have excellent electron percolation pathways. Comparative studies in TiO_2 have shown that highly ordered, vertically oriented nanotube arrays outperform colloidal counterparts in applications such as sensors, water photoelectrolysis, dye-sensitized, and solid-state heterojunction solar cells, and photocatalysis. Biosensors, molecular filtration, drug delivery, and tissue engineering are just a few of the biomedical applications where they have shown remarkable properties. The use of nanoporous alumina templates, sol-gel preparation using organo-gelator templates, seeded growth mechanisms, and hydrothermal techniques have all been used to make TNAs. By optimizing various parameters such as pH, concentration, and composition of the electrolyte, applied potential, time, and temperature of anodization, fabrication of oxide nanotube arrays by electrochemical anodization of the starting metal offers superior control over nanotube dimensions. (D. Pathinettam Padiyan, 2012).

2.6.3 Effects of Fabrication Factors on TNAs

2.6.3.1 Electrolyte

The first and most widely studied electrolyte in titanium anodization to produce TiO₂ nanostructures is hydrofluoric acid (HF). Since then, several optimized electrolytes of various acid/HF mixed electrolytes have been proposed for successful TiO₂ nanostructure fabrication (R. Beranek, 2003). Table 2.3 provides a summary of the various TNA synthesis generations. However, in this first synthesis generation, the nanotube length is limited to a few hundred nanometers. This second generation of TNAs was produced in a neutral electrolyte containing fluoride ions, such as Na₂SO₄/NaF or (NH₄)₂SO₄/NH₄F, with a remarkably high aspect ratio. The limited dissolution on the top of nanotubes in the neutral electrolyte is the cause of the tube length increase. Due to current oscillations during the anodization process, the nanotubes produced by the above inorganic electrolyte always had a rough external structure, such as "rings" or "ripples." Organic electrolytes with fluoride salt additions, the third-generation electrolyte, allow the construction of smooth and much taller TNAs in the hundreds of micrometer range. Inorganic viscous electrolytes, the longest tube lengths to date have been up to 1000 m. The morphology, structure, and growth rate of the as-formed TiO₂ nanotube are all influenced by the pH of the electrolyte and the amount of water present. TNAs have recently been synthesized using fluoride-free electrolytes, which is referred to as the fourth generation. The result of this rapid breakdown anodization (RBA) is also a bundle of disordered nanotubes that grow in a matter of minutes. (R. Hahn, 2007) Each electrolyte provides a unique geometrical feature of the nanotubes and thus varying surface properties, depending on the electrolyte nature; thus, selecting an electrolyte medium for TNA fabrication is a primary concern.

Table 2.3 Summaries of various synthesis generations of TNA's

Generation	Electrolyte type	Potential	Anodized time	Morphology	Main factor	Reference
<i>First generation:</i> inorganic aqueous electrolytes (HF-based electrolyte)	0.5 wt% HF	10–23 V	≥20 min	Short nanotubes Length: 200–500 nm Diameter: 10–100 nm Wall thickness: 13–27 nm	Potential, electrolyte	D. Gong 2001
	0.3–0.5 wt% HF + 1 M H ₃ PO ₄	1–25 V	2h	Length: 20–1000 nm Diameter: 15–120 nm Wall thickness: 20 nm		S. Bauer, 2006
<i>Second generation:</i> buffered electrolytes (F ⁻ -based electrolytes)	1 M Na ₂ SO ₄ + 0.1–1.0 wt% NaF	20V	10 min–6 h	Diameter: 100 nm Wall thickness: 12±2 nm	Potential, pH, time	J. M. MacAk, 2005
	1 M (NH ₄) ₂ SO ₄ + 0.5 wt% NH ₄ F	20V	15–30 min	Length: 0.5–1.0 μm Diameter: 90–110 nm		
<i>Third generation:</i> organic electrolyte	0.5 wt% NH ₄ F + 0–5 wt% H ₂ O in glycerol	20V	13h	Smooth tube Length: 7.0 μm	Potential, water content, time	J. M. Macak, 2005

containing F ⁻ ions				Diameter: ≈40 nm Wall thickness: 12±2 nm		
	0.1–0.7 wt% NH ₄ F + 2–3.5 wt% H ₂ O in ethylene glycol	60V	216h	Ultra-long tube Length: 1000 μm Diameter: 120±10 nm		M. Paulose, 2007
<i>Fourth generation:</i> fluoride-free electrolytes	0.01–3 M HClO ₄	1 min	15–60 V	Disordered tubes Length: 30 μm Diameter: 20–40 nm Wall thickness: 10 nm	Electrolyte, time	R. Hahn, 2007

2.6.3.2 Voltage

The morphology of formed nanostructures is influenced by the anodization voltage: at low voltages of 5 V, pores instead of tubes grow, while at voltages higher than 8 V, the diameter of TiO₂ nanotubes is also influenced linearly by the applied voltage. Breakdown events can be observed inside the nanotube at high anodization voltages (>50 V), resulting in sponge-like structures. Electropolishing of the samples would occur at a high current density (>100 mA cm²) in this electrolyte at even higher anodization voltages (>80 V). As a result, delaying the occurrence of breakdown events is critical for the creation of a larger tube diameter. TNAs with a diameter of about 600 nm were obtained in ethylene glycol electrolytes containing 0.09 M ammonium fluoride and 10 % water, according to Yin et al. (H. Yin, 2010). Albu and Schmuki increased the tube diameter to 800 nanometers. These tubes, on the other hand, do not appear to be well-organized and appear to be loosely assembled in a mesoporous matrix rather than in a well-defined nanotube array. (Schmuki, 2010) Using a higher voltage regime of up to 225 V, Ni et al. successfully demonstrated well-defined, large diameter (680–750 nm) TNAs with the most uniform and clean morphology.

2.6.3.3 Anodization Time and Step

The effect of the first step anodization time on the morphology of TNAs grown by two-step anodization and their photocurrent response in dye-sensitized solar cells with backside illumination by increasing the first step anodization time, a significant increase in tube order will show. For a range of first step anodic oxidation from 0.5 to 6 h, the fill factor and open-circuit voltage of all dye-sensitized solar cells were approximately 60% and 0.77 V, respectively, whereas the short circuit current increased from 0.94 to 1.57 mA/cm², leading to a 73 % increase in photo-to-current efficiency. We attributed the improved cell performance to lower recombination rates due to higher ordered TNAs associated with the actual surface area and coherency of the cells' components, as determined by open-circuit voltage decay and electrochemical impedance spectroscopy (the Nyquist and Bode plots).

2.6.3.4 Fluoride Concentration

The electrodeposition of LaF₃ on synthesized TNAs was used to make TNA electrodes. Scanning electron microscope (SEM), X-ray diffraction (XRD), and energy

dispersive X-ray spectrometer were used to examine the electrode (EDS). The electrode had a good response to the fluoride ion. The electrode's sensitivity is higher than that of ordinary fluoride ion-selective electrodes, and the linear calibration range achieved four orders of magnitude of F⁻ concentration (10⁶–10² mg/ml) (mode PF-1). The detection limit (LOD) was calculated to be 4.39 10⁷ mg/ml (S/N = 3). The new electrode was used to measure traces of fluoride ions in tap water and toothpaste. Finally, fluoride in milk samples was determined using a headspace single-drop microextraction (SDME) system and a LaF₃/TNAs electrode. With an average relative standard deviation (RSD percent) of 0.51 % and a recovery rate of 96.3 % to 107.3 %, the results are satisfactory (Bin Zhang, 2012).

2.6.3.5 pH and Temperature

TNAs are a promising photocatalyst for removing micropollutants from water, but more research is needed to understand their applicability in complex water matrices. This research looks into the impact of dissolved natural organic matter (NOMs) on TNA's ability to remove 4-chloro-2-methylphenoxyacetic acid (MCPA, a common micropollutant found in many water bodies). Although NOMs undergo photosensitization in the bulk liquid phase, which can aid in MCPA removal, the overall effect of NOMs on MCPA removal is negative due to the interaction between NOMs and the TNA surface: total MCPA removal decreased from 94.3 % to 62.0 % and 61.8 %, respectively, in the presence of only 5 mg/L SWR-NOM and UMR-NOM. In the presence of 15 mg/L SWR-NOM and UMR-NOM, acidic pH was found to be able to mitigate the detrimental effect of NOMs (total MCPA removal was only reduced from 94.5 % to 83.3 % and 88.8 % under acidic pH, respectively), and the photosensitization effect of NOMs was strengthened; however, under alkaline pH conditions, the detrimental effect of NOMs completely vanished. Phosphate and bicarbonate, two commonly found co-existing anions, also help to mitigate the negative effects of NOMs. With 15 mg/L SWR-NOM, the addition of 100 mg/L bicarbonate increased total MCPA removal from 49.1% to 65.1 %; the addition of 100 mg/L phosphate increased total MCPA removal from 49.1% to 62.5 %. The presence of 100 mg/L bicarbonate increased total MCPA removal from 45.2 % to 56.1 % with 15 mg/L SWR-NOM; the presence of 100 mg/L phosphates increased total MCPA removal from 45.2 % to 62.9 %. The photocurrent measurements show that the presence of such anions significantly reduces the h⁺ scavenging effect of

NOMs, whereas other anions, such as chloride, nitrate, and sulfate, have no effect (Yin Yea, 2019).

2.7 Application of TNAs

2.7.1 Photocatalyst

TiO₂ is an n-type semiconductor, has gotten a lot of coverage after Fujishima and Honda discovered it could decompose H₂O under illumination in 1972. TiO₂ has several unique properties, including low toxicity, ease of fabrication, low cost, high stability, and excellent photosensitivity. As a result, it is commonly used in photodegradation of organics, photocatalytic water splitting, dye-sensitized solar cells, gas sensors, photoelectrochemical cathodic safety (also known as photocathodic protection), biomedical materials, and other fields. A vertically focused anatase TNAs film prepared by a simple electrochemical anodization process has higher photoelectrochemical activity than a TiO₂ nanoparticle or nanowire film due to its wide interfacial region and excellent electron-transport property. However, TiO₂ has a wide bandgap of 3.2 eV and can absorb only UV radiation, which accounts for only a limited portion of sunlight. Furthermore, the photogenerated charge carriers in TiO₂ quickly recombine, reducing TiO₂'s photoelectrochemical efficiency (Zi-Chao, Hai-Peng, Xia, Juan, & Rong-Gui, 2018).

An ideal photocatalyst should be photon-activated, chemically inert, readily accessible, nontoxic, and capable of using a large solar spectrum. The disparity in energy between VB and CB is known as the bandgap, and it determines if the substance is a conductor, a semiconductor, or an insulator. In contrast to insulators and metals, semiconductors have a bandgap that allows them to produce electron (e⁻)/hole (h⁺) pairs as they absorb a photon with energy equal to or greater than their bandgap. Because of their desirable bandgap and band edge positions, semiconducting metal oxides are widely used as photocatalysts. The electronic structure of semiconductors is important since the VB of the semiconductor is packed with electrons while the CB is empty. The bandgap of various semiconductor materials varies depending on their electrical configuration. Table 2.3 shows some of the bandgaps of semiconductor oxide materials (Milind, S., & Perena, 2018).

Table 2.4

Bandgap energies of semiconductors as photocatalyst.

Photocatalyst	Bandgap energy (eV)
ZrO ₂	5.0
ZnS	3.6
TiO ₂ (anatase)	3.2
TiO ₂ (rutile)	3.0
WO ₃	2.8
SnO ₂	2.5
Fe ₂ O ₃	2.3
GaP	2.25
V ₂ O ₅	2.6
CuO	1.7
CdSe	1.7
MnO ₂	0.25
CeO ₂	2.94

Source: (Milind, S., & Perena, 2018).

Table 2.4 depicts the fundamental mechanism of semiconductor photocatalysts (TiO₂, ZnO, ZnS, and Fe₂O₃). As seen in Table 2.4, when a photon with sufficient energy (the semiconductor's bandgap energy) is consumed by the semiconductor, an electron from the VB is excited and leaps to the CB, resulting in a hole in the valence band. Photoexcitation is the method of generating electron-hole pairs. Photoexcited electrons can be used to reduce oxygen, and holes can be used to oxidize water molecules that are adsorbed on the photocatalyst surface (Milind, S., & Perena, 2018).

TNTs can be made using a variety of techniques. Electrochemical anodization, on the other hand, provides a simple and more durable method of producing TNTs at a low cost. Furthermore, TNTs can be grown on titanium substrates, resulting in high surface

area materials that improve the interface between gas and nanostructures while still having an immobilized characteristic. While this method has many benefits, there could be some problems with the reproducibility of the prepared samples. The photocatalytic efficiency of TNTs is highly dependent on their surface morphology. TNTs surface morphology is influenced by several experimental factors, including anodization time, anodization potential, and electrolyte composition. The nanotubes' calcination temperature is another important factor that influences the nanotubes' properties and the photocatalyst's reaction efficiency (Nurul, Rab, Chong, Siew, & Mohd, 2020). Furthermore, the TiO₂ anodized using the two-step method exhibits improved adhesion of the grown tubes to the substrate as well as the benefit of having open-ended tubular bottoms fixed to the wall, which significantly mitigated the major problems encountered by the traditional tubes grown using the one-step method. The findings and review section includes a thorough review of the comparative discrepancies between the two approaches (Tenzin, dll., 2018).

Many posttreatment processes, such as annealing in a specific gas atmosphere, hydrothermal treatment, and vapor-thermal treatment, have been widely used to synthesize special crystallized TNAs with high system efficiency. Annealing the anodic TNAs in a sealed container with unique conditions, such as oxygen-rich (O₂), oxygen-deficient (Ar, N), and other reducing (H₂) gas, will change the crystal structure, morphology, and electronic properties of the TNAs and affect their photocatalytic efficiency. However, this approach is costly and uses a lot of resources. Recently, significant work has been devoted to the creation of hierarchical architectures based on 1D TNAs nanostructure models. For example, a simple hydrothermal treatment was used to reduce the heat treatment temperature for the construction of anatase TiO₂ nanostructures as a result of a dissolution recrystallization transformation of amorphous anodic TNAs, and the resulting hierarchical TiO₂ structures decorated with TiO₂ nanoparticles have a larger surface area than smooth TNAs, demonstrating an enhanced surface area (Warapong, dll., 2013). In comparison to heteroelement doping (e.g., N, F, and C) of TNAs, in situ self-doping with homo species (e.g., Ti³⁺, and H⁺) using an electrochemical reduction procedure has recently emerged as a reasonable solution to improve TiO₂ photoactivity in both UV and visible light regions. Despite significant contributions from several communities, well-designed post-treatment techniques for constructing desired crystalline structures with high surface area and anatase process for

highly efficient pollutant degradation remain an appealing ongoing challenge (Jiaguo, Gaopeng, & Bei, 2010).

2.7.2 Solar Cells

2.7.2.1 Dye-Sensitized Solar Cells (DSSCs)

DSSC is built on photoanodes, which are oxides with large bandgaps such as TiO₂, ZnO, SnO₂, and others. Dye sensitization, transition metal ion doping sensitization, inorganic narrow bandgap semiconductor sensitization, and other approaches are used to create it. Because of advantages such as low preparation cost, lightweight materials, good processing efficiency, and a wide design area of the compound structure, DSSC is more promising for commercialization than other solar cells. Currently, porous TiO₂ thin films are commonly used to prepare a DSSC photoanode. Simultaneously, the preparation of one-dimensional nanomaterials has three benefits:

- i. Improving the specific surface area by decreasing the nanotube diameter and increasing the tube length - titanium dioxide nanotubes with a broad specific surface area are advantageous for the successful adsorption of dyes with low absorption coefficients (such as the N-719):
- ii. A strong electrical interaction is formed between the components, resulting in a higher open voltage by reducing the composite loss during electron transport; and
- iii. One-dimensional materials increase electron lifespan, resulting in a greater oxidation time (Zao, dll., 2019).

2.7.2.2 Quantum Dots Sensitized Solar Cells (QDSSCs)

Semiconductor quantum dots (QDs) such as CdX (X = S, Se, Te), PbX (X = S, Se, Te), CuInX₂ (X = S, Se), and others have been widely used as sensitizers for solar cells due to their specific properties of tunable bandgap, strong absorption coefficient, ultrafast electron transfer, quantum size-effect, and multiple exciton production. The photovoltaic conversion efficiency of QDSSCs has already surpassed 12% by various processes such as chemical bath deposition, successive ionic layer adsorption and reaction, co-sensitization, surface passivation treatment, and so on. Unfortunately, as third-generation solar cells, QDSSCs have a potential photovoltaic conversion efficiency

of 44%, which is a significant difference as compared to recent records. The optical absorption property of the photo-electrodes in the QDSSCs device is a significant factor for the charge generation content of QDSSCs, which is primarily determined by the instinctive optical absorption potential of QDs. Many studies have been conducted over the last decade to boost the charge generation content of QDSSCs using innovative processes such as size-effect modulation, co-sensitization, alloyed processes, and so on. While the optical absorption property of QDSSCs has been vastly improved across the entire ultraviolet and visible light field, including the near-infrared light region, the charge generation content of QDSSCs also needs to be improved. The optical absorption property of the QDSSCs has not been reached at the optimum condition due to the comparatively low deposition of QDs in the QDSSCs device, which is a significant problem to remember. The QDs deposition method, as we know, determines the QDs deposition material in the QDSSCs framework. And several novel QDs deposition methods, such as the assembly linking process, electrodeposition process, and so on, have been developed, effectively improving the deposition quality of QDs and achieving one of the champion power conversion efficiency for the QDSSCs. However, the optimal charge generation material has yet to be realized. The charge recombination effect is still present in certain areas of photo-electrodes. As a result, it is critical to increase the deposition content of QDs and the charge transfer rate in QDSSCs even further (Zhuoyin, dll., 2020).

2.7.3 Water Splitting

TNAs are considered ideal candidates for highly efficient water splitting because the theory of photoelectrolysis for water splitting is the same as that of photocatalysis (see Table 5). The photoelectrolysis method using TiO₂ nanotube cells as a photoanode is as follows: when the photoanode is immersed in water and subjected to light irradiation, it absorbs photonic energy above its bandgap energy, resulting in the generation of electron-hole pairs. The produced holes oxidize O²⁻ ions from absorbed water, producing oxygen gas as well as an electric current that flows through the external circuit to the conducting cathode, where it reduces H⁺ ions to create hydrogen gas. TNAs prepared by titanium anodization have recently sparked a lot of interest in photocatalytic water splitting. The hydrogen production rate of 96 μmol/h/cm² by using a nanotube array (224 nm in length) for water splitting with a steady voltage bias of 0.4 V (versus Ag/AgCl).

The recently registered a 150 $\mu\text{mol/h/cm}^2$ hydrogen generation rate by three-step electrochemical anodized TNAs with a normal porous top layer. Furthermore, under 320 mW/cm^2 irradiation, palladium quantum dots sensitized TNAs demonstrated a highly effective photocatalytic hydrogen output rate of 592 $\mu\text{mol/h/cm}^2$. In general, the rate of hydrogen production is highly influenced by the electrolyte, external bias, light strength, and morphology and structure of TiO_2 . As a result, it is critical to refine these parameters and fundamentally consider their potential associations to simplify approaches to building high-efficiency cells for hydrogen generation (Jianying, Keqin, & Yuekun, 2015).

Table 2.5 Summary of TNA-based materials in water splitting

Photoanode	Light intensity (mW/cm^2)	Electrolyte	Photocurrent (mA/cm^2)	Water splitting ($\mu\text{mol/h/cm}^2$)
C-TNTs	N/A; 500 W Xe lamp	0.1 M Na_2S and 0.02 M Na_2SO_3	N/A	1.6 (0.040 mL/h/cm²)
TNT	70; 300 W Xe lamp	1 M KOH	0.58 @ 0.6 V vs. NHE	7.1 (0.178 mL/h/cm²)
C-TNT (C-containing TiO_2 -based nanotube arrays)	12.7, 300 W Xe Lamp	1 M KOH	1.96 @ 0 V vs. Ag/AgCl	11.28 (0.282 mL/h/cm²)
TiO_2 nanotubes with anything pretreating	87, 300 W AM 1.5	1 M KOH	1.78 @ 1.23 V RHE	(0.87 mL/h/cm²)
Ru/ TiO_2 nanotube @ 0.05 at. % Ru	100	1 M KOH	1.78 @ 0.4 V vs. Ag/AgCl	45 (1.08 mL/h/cm²)
TiO_2 nanotubes (224 nm length, 34 nm wall thickness)	100	1 M KOH	13.0 @ 0 V vs. Ag/AgCl	96 (2.30 mL/h/cm²)

TiO ₂ nanotubes	110	1 M KOH and 0.5 M H ₂ SO ₄ electrolytes	4.95	97 (2.32 mL/h/cm ²)
TiO ₂ nanotubes	74	1 M KOH	N/A	140 (3.28 mL/h/cm ²)
Leaflike TiO ₂ /TiO ₂ nanotubes	320	2 M Na ₂ CO ₃ + 0.5 M ethylene glycol	16.3 @ 0.9 V vs. SCE	150 (3.39 mL/h/cm ²) @ -0.3 V vs. SCE
<i>Pyrococcus</i> <i>furius</i> /TiO ₂ nanotubes	74	1 M KOH	N/A	234.88 @ 1.5 V vs. Ag/AgCl
TiO ₂ nanotubes	74	1 M KOH	32.8 @ 1.5 V vs. Ag/AgCl	250
TiO ₂ nanotubes (three-step anodization)	320	2 M Na ₂ CO ₃ + 0.5 M ethylene glycol	24 @ -0.3 V vs. SCE	420
Pt@TiO ₂ nanotubes	320	2 M Na ₂ CO ₃ + 0.5 M ethylene glycol	24 @ -0.3 V vs. SCE	495
Pd@TiO ₂ nanotubes	320	2 M Na ₂ CO ₃ + 0.5 M ethylene glycol	24 @ -0.3 V vs. SCE	592

Source: (Jiaying, Keqin, & Yuekun, 2015).

2.7.4 Other Applications

The electrochemical decomposition of lipopolysaccharide (LPS) was first studied using a TNAs electrode. The TNTs layer of this electrode was made up of various tubular structures that were closely packed together, with an average diameter of 100 5 nm for each nanotube. LPS and polysaccharides degraded using pseudo-first-order kinetics. The optimum LPS removal ratio was close to 80%. During the electrolysis step, the endotoxin toxicity of LPS gradually decreased. The acute toxicity of the intermediates increased abruptly (5 min) at the start of the electrochemical degradation process, then retained a high inhibition ratio (> 95 percent) for about 150 minutes, and then decreased slightly (

10%) after electrolysis for 240 minutes. LPS with a molecular weight of 116,854 Da was converted into small molecular compounds with molecular weights ranging from 59,312 to 12,209 Da after 20 minutes of electrolysis. Electric-field-force-driving aggregation, adsorption, and direct electron transfer on TNAs electrodes, and $\bullet\text{OH}$ oxidation were suggested as possible LPS degradation and detoxification mechanisms (Kaixuan, dll., 2020).

Electrochemical anodized TNTs are extremely important as electrochemical energy storage devices because they allow for rapid electron transfer by shortening the diffusion path and paving the way for the fabrication of binder-free and carbon-free electrodes. Aside from these benefits, doping the lattice with nitrogen doubles its electrochemical operation due to improved charge transfer caused by oxygen vacancy. We synthesized nitrogen-doped TiO_2 (N- TiO_2) and investigated its electrochemical properties in a supercapacitor and as an anode for a lithium-ion battery in this study (LIB). Raman spectroscopy and X-ray photoelectron spectroscopy (XPS) techniques were used to validate nitrogen doping in TiO_2 . The electrochemical output of N- TiO_2 nanotubes as a supercapacitor electrode was excellent, with a basic capacitance of $835 \mu\text{F cm}^2$ at 100 mV s⁻¹ scan rate, and areal discharge power of $975 \mu\text{Ah cm}^2$ as an anode material for LIB, which is far superior to bare TNTs (505 F cm^2 and $86 \mu\text{Ah cm}^2$, respectively). This custom-made nitrogen-doped nanostructured electrode holds great promise as a material for next-generation energy storage electrodes (Tamilselvan, Chandrasekar, Rajesh, Smagul, & Balakumar, 2019).

TNA uses can be greatly extended if secondary material can be effectively deposited into the tubes. TNAs may also be transformed to other titanates MTiO_3 (M = Sr, Pd, Zr) with unique bioactive, piezoelectric, or ferroelectric properties while retaining their original tube structure through a simple hydrothermal process in the corresponding precursor solution or a direct anodizing process on suitable alloy substrates (Jian-Ying, Ke-Qin, & Yue-Kun, 2013).

2.8 Summary of Literature Review

From semiconductor photocatalysts to photoreactors for photocatalytic CO_2 reduction, a thorough literature review has been conducted. The tri composite photocatalyst used in this analysis has never been used for photocatalytic CO_2 reduction.

The rapid rise in CO₂ GHG levels in the atmosphere poses a threat to humanity. Furthermore, the loss of fossil fuels causes a major crisis in global fuel production as well as total electricity demand. However, photocatalytic CO₂ conversion using a plentiful supply of photon energy from solar light and a readily available semiconductor photocatalyst may be a fruitful option for both energy and environmental solutions. Furthermore, many factors hinder the vast range of practical implementations that might make this method a success. These research holes can be filled by using novel photocatalysts, as well as implementing and modifying the photoreactor to achieve the desired process performance.

CHAPTER 3

METHODOLOGY

3.1 Flowchart of Methodology

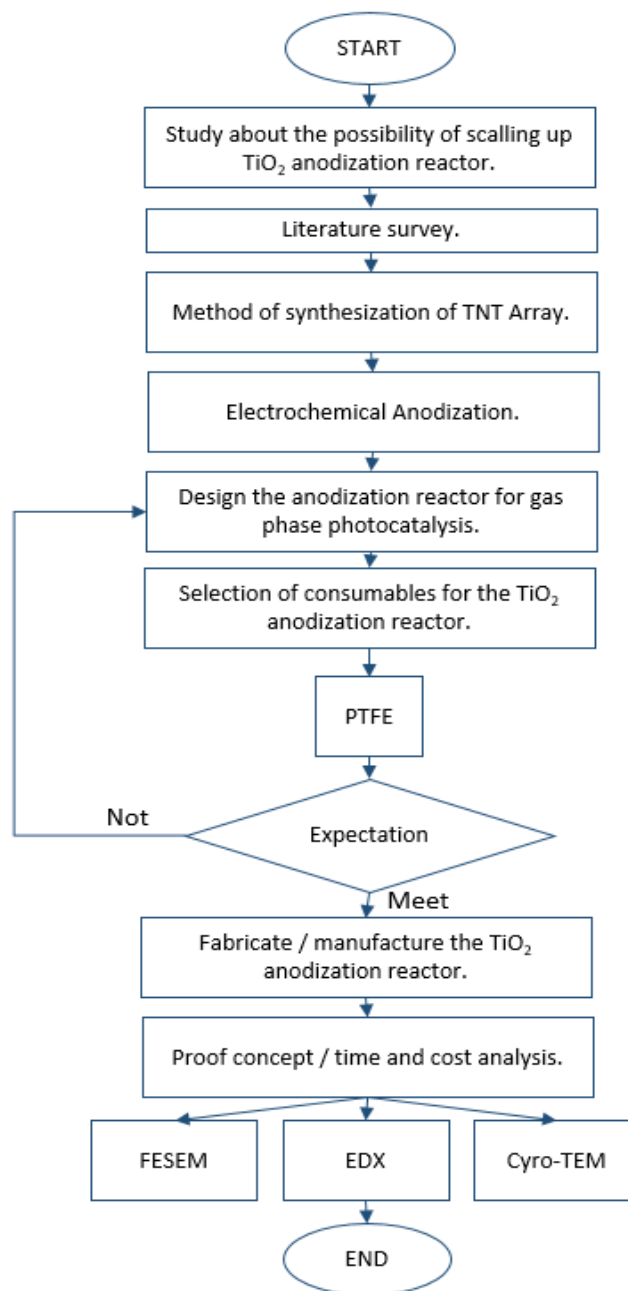


Figure 3.1 Flowchart

3.2 Design of Anodization Device

Design Rationales. While designing the new anodization device, the design rationales of the device setup were initially evaluated, followed by proof of concept data, leading to further upscale and optimization. Design rationales included the following:

- i. To create a scalable device design that was suitable for multiple specimens per batch of the anodization process;
- ii. Maintain constant electrode distances for process control;
- iii. Ensure device setup that was compatible with the use of hydrofluoric acid (HF);
- iv. Allow an even distribution of potential and current to all specimens;
- v. Allow monitoring of the potential of the working electrode during the anodization process;
- vi. Include a counter electrode that was at least similar or larger area to that of the working electrode;
- vii. Allow no contamination from copper parts, which deleteriously affects the anodizing process;
- viii. Allow manufacture of a specimen shape that maximizes the surface area; and
- ix. Allow ease of use when transferring the specimens.

3.3 Consumables Selection

A Polytetrafluoroethylene (PTFE) beaker was employed to contain the electrolyte as PTFE is resistant to HF, as compared with glass or other plastic materials like low-density polyethylene (LDPE), high-density polyethylene (HDPE), polypropylene (PP), polymethyl pentene (PMP), and styrene-acryl (SAN). The PTFE beaker can also be autoclaved under high temperature if needed. The holder for the working electrode was a copper rod (shielded by PTFE and lacquer masking to prevent copper from exposing to the electrolyte) to which specimens were attached. Anodization was able to take place over the entirety of the specimen, and the specimen shape could be varied according to the application.

3.4 Manufacturing of Anodization Device

The platinum counter-electrode was attached to a shielded copper rod holder. The counter-electrode was positioned 40mm from the working electrode holder. Two square platinum foils (50mm× 50mm) were welded to provide an electrode of area approximately 94mm× 50 mm. The reference electrode was placed close to the working electrode to monitor potential changes across the systems. Lacquer was used to seal connections of the platinum and specimens to the copper rods. The top cover jig of the device permitted the electrode arrangements to be preserved between batches. An opening in the cover jig allowed access to air.

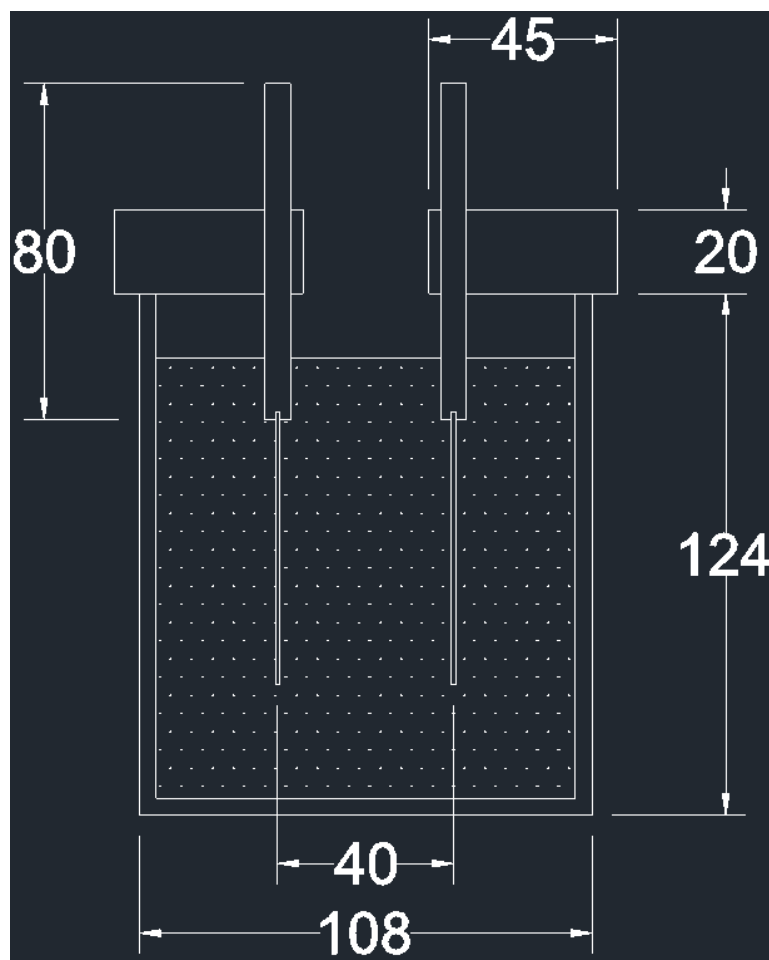


Figure 3.2 Proposed design with dimension.

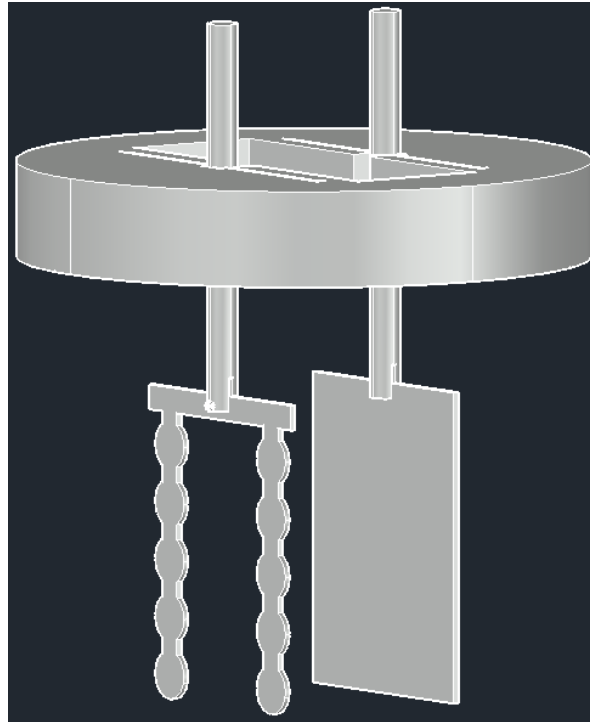


Figure 3.3 Proposed design for upscale anodization device.

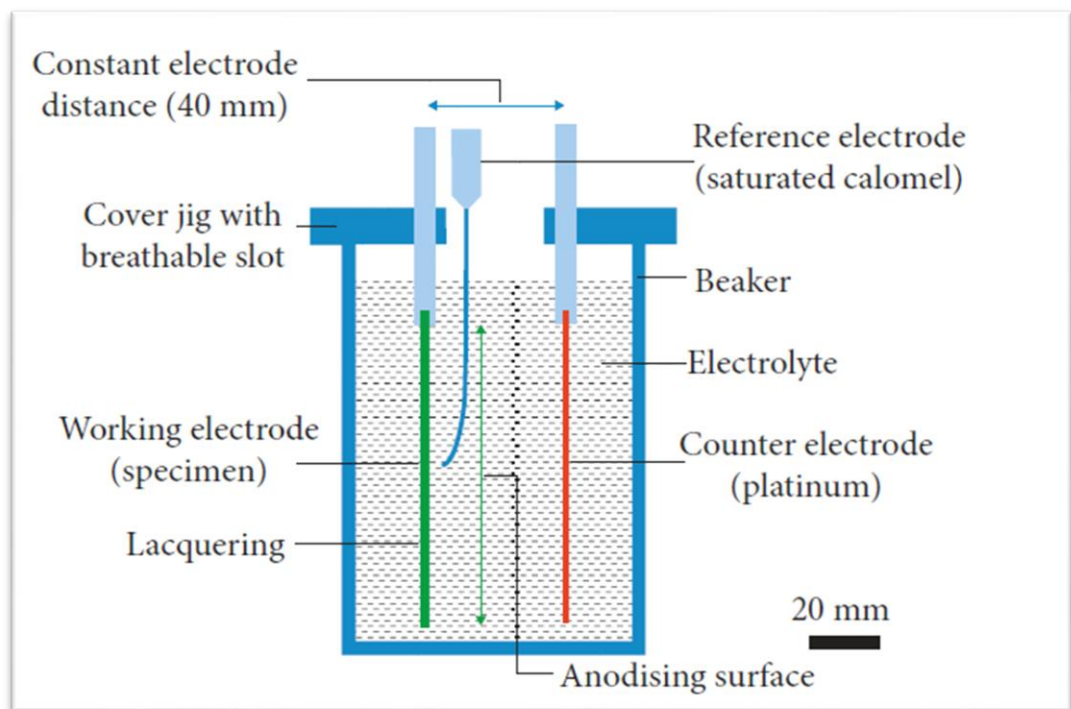


Figure 3.4 The schematic diagram of an up-scale anodization device.

3.5 Proof Concept

10 wire-cut electrical discharge machining (EDM) connected specimens were anodized. The illustrations could be separated later by cutting the connecting strips between the discs provided by the metal sheet cutting procedure. The resulting tags on each disc could be folded into an L shape to ease the transference of specimens without damaging the specimen surface. The number of samples was limited to 10 to be compatible with the output of the power supply. Three (3) analyses will be done for TNTs prepared by the new anodization reactor. Type of analyses are:

- i. Field Emission Scanning Electron Microscopy (FESEM);
- ii. Energy Dispersive X-Ray Spectroscopy (EDX); and
- iii. Cryogenic Transmission Electron Microscopy (Cryo-TEM)

3.5.1 Field Emission Scanning Electron Microscopy (FESEM)

The Field Emission Scanning Electron Microscope (FESEM) allows ultra-high resolution imaging at low accelerating voltages and short working distances. A new FESEM imaging facility, the GeminisSEM 500, will be deployed soon in MTEC, BTI. It delivers picture resolution as low as 0.6 nm at 15 kV and 1.2 nm at 1 kV, allowing the study of the top surface of nanopowders, nanofilms, and nanofibers in a variety of applications, including mineralogy, ceramics, polymer, metallurgy, electrical devices, chemistry, physics, and life sciences. This system includes many detectors for detecting different signals, such as a secondary electrons (SE) sensor for topographic information and a back-scattered electrons (BSE) detector for material composition comparison. EDS with a detector energy resolution of 129 eV and a detection limit in the range of 1000-3000 ppm coupled with FE-SEM is used to evaluate the chemical composition of micro-features ranging from boron (B) to uranium (U). WDS, which has a detector resolution of 2-20 eV and a detection limit of 30-300 ppm when paired with FESEM, is used to identify elements that EDS cannot resolve. The combination of ultra-high-resolution imaging with high-sensitivity WDS aids in determining thorium and rare earth elemental analysis (Cik Rohaida , dll.).

3.5.2 Energy Dispersive X-Ray Spectroscopy (EDX)

Energy Dispersive X-ray (EDX) microanalysis is an elemental analysis technique related to electron microscopy based on creating specific X-rays that indicate the existence of elements present in specimens. Many researchers and physicians employ EDX microanalysis in several biomedical domains. Nonetheless, the majority of the scientific community is unaware of its potential uses. The EDX microanalysis spectrum provides both semi-qualitative and semi-quantitative information. The EDX methodology is being used in the research of pharmaceuticals, such as medication delivery. The EDX is an essential instrument for detecting nanoparticles (generally used to improve the therapeutic performance of some chemotherapeutic agents). EDX is also used to investigate environmental contamination and to characterize mineral bioaccumulation in tissues (Manuel, Simone, Rita, Harpreet, & Elena, 2018).

3.5.3 Cryogenic Transmission Electron Microscopy (Cryo-TEM)

Cryogenic transmission electron microscopy (Cryo-TEM) may be used to image nanoscale objects floating in liquid media directly. Cryo-TEM has been utilized successfully in microbiology and other biological domains. Samples are made by immersing a thin layer of the work in a suitable cryogen, which creates a photograph of the suspended items in their liquid medium. With proper sample preparation, Cryo-TEM pictures can aid in understanding aggregation and self-assembly and give specific information about cells and viruses (Nathan & R., 2013).

CHAPTER 4

RESULTS AND DISCUSSION

4.1 The Differences between the Lab Scale and The Up-Scale of The Reactor Design

An electrochemical technique that turns a metal surface into an attractive, durable, corrosion-resistant anodic oxide finish is known as anodization. Anodizing is done by immersing aluminum in an acid electrolyte bath and then passing an electric current through it. The inside of the anodizing tank has a cathode, and the aluminum functions as an anode, allowing oxygen ions from the electrolyte to react with the aluminum atoms on the surface of the component being anodized. As a result, anodizing is a process of highly controlled oxidation that enhances a naturally occurring phenomenon (Aluminum Anodizers Council, 2017).

Regular anodization is commonly used, such as lab beakers, Titanium anode, Platinum cathode, and DC power supply. Some advanced setup using magnetic stir plate and temperature control system to run the anodization smoothly. But for the up-scale anodization have some additional apparatus such as:

- i. Liquid supply pump, single head, cycling;
- ii. PH testing and controller;
- iii. Electrode rack; and
- iv. Reactor tank using Polypropylene, PP materials.

The liquid supply pump is used as an auto-fed electrolyte to maintain the amount of the electrolyte in the reactor tank. The electrolyte will slowly be consumed over time, and also the top-up system based on the pH meter. The electrolyte can be top-up based on PH setting value. Next is the electrode rack is used as a holder for the electrode inside the reactor tank. And lastly, the material for the reactor tank uses PP because it has good resistance before being eroded.

4.2 The Selection for Fabricate Factors of Effects

The selection for fabrication is important because different materials will produce different results. Several fabrication factors must be considered in this experiment such as:

- i. Electrode material;
- ii. Electrolyte;
- iii. Voltage Apply;
- iv. Anodization Time; and
- v. Temperature.

4.2.1 Working Electrode Anode

In an electrochemical system, the working electrode is where the reaction of interest occurs. The active electrode is classified as cathodic or anodic, depending on whether the response on the electrode is reduction or oxidation. Inert metals like gold, silver, or platinum, inert carbons like glassy carbon, boron-doped diamond, pyrolytic carbon, and mercury drop and film electrodes are common working electrode materials (James, 2000).

As a result, in this up-scale electrochemical anodization, the primary material that must be used to convert carbon dioxide (CO_2) into methane (CH_4) is titanium oxide nanotubes (TNTs) which must be used as the working electrode at the anode. Because the material would have a well-defined, honeycomb-like tubular structure with thin walls, Ti-6Al-4V was chosen (Ribeiro, et al., 2021).

4.2.2 Counter Electrode Cathode

The counter electrode, also known as an auxiliary electrode, applies input potential to the working electrode. These electrodes are responsible for completing the circuit and allowing charge to flow. As a result, they must be made of an inert substance like carbon or platinum. To avoid current limits, their size must be significantly more significant than the working electrode. (Honeychurch, 2012).

The cathode's overpotential is a significant component that impacts the Ti anode's dissolution kinetics, which controls the activity of the electrolyte and the morphology of the produced TNTs. The greater the dissolved Ti in the electrolyte, the higher the conductivity of the electrolyte, which helps to reduce debris formation. Due to variances in their overvoltage inside the test electrolyte, different cathode materials appear to have produced diverse morphologies. As a result, the cathode materials are arranged in the following order based on their aqueous electrolyte stability (Indira, Mudali, & Nishimura, 2015).



For the up-scale, the graphite or carbon material has been used because of the low cost and high stability compared to others.

4.2.3 Electrolyte

Any material that ionizes when dissolved in water or ionizing solvents is an electrolyte. Almost all soluble acids, bases, and salts fall within this category. When there is low pressure or a high temperature, gases like hydrogen chloride can operate similarly to electrolytes. Because their presence causes a reaction between two dissimilar metals, electrolytes are essential in corrosion (Corrosionpedia, 2018).

The type of electrolyte used in the production of TNTs has a significant impact on the establishment of the graded structure. It was commonly recognized that various electrolytes could create varied electric field intensities under the same circumstances. It was also well known that in the early stages of anodization, a higher electric field strength can produce more significant breakdown sites, resulting in a larger TNTs diameter. In addition, the chemical dissolution rate of the oxide layer varies depending on the electrolyte. In other words, by changing the electrochemical anodization parameters of Ti, one may generate various titanium oxide structures such as a flat compact oxide, a disordered porous layer, a highly self-organized porous layer, and a highly self-organized nanotubular layer.

The TNTs can be made by anodizing fluoride-containing electrolytes such as $\text{NH}_4\text{F}/\text{CH}_3\text{COOH}$, $\text{H}_2\text{SO}_4/\text{HF}$, $\text{Na}_2\text{HPO}_4/\text{NaF}$, and so on. The electrolytes utilized have a significant impact on the diameter of nanotubes. In this particular experiment for up-scaling the TNTs, the $\text{NH}_4\text{F}/\text{CH}_3\text{COOH}$ electrolyte was been choose.

4.2.4 Voltage Apply

The applied voltage has various effects on pore diameter, interpore distance, and film thickness. As a result, the applied voltage and anodization duration significantly impact the layer's shape. Tubes of a few hundreds of nanometers in length and a few tens of nanometers in diameter were created at low applied voltages. Rings join individual tubes on the sidewalls of the tubes in short-term anodization, but tubes are separated in longer-term anodization due to the breakdown of these rings (Kim, Fujimoto, Schmuki, & Tsuchiya, 2008).

At a voltage of 20 V, the most stable porous structure is formed. Nanopores are present in films generated at potentials below 20 V, although the structures are thinner. The layers do not thicken anymore in this situation because the current is insufficient. The films generated between 22 and 30 V have a tubular yet irregular porous structure. Large broken regions of a porous oxide film with a diameter in the micrometer scale developed at the interface film substrate over 30 V, which may be linked to breakdown events at high potentials. The morphology of the porous film is comparable to porous alumina at low anodizing voltages (Gong, et al., 2011).

4.2.5 Anodization Time

The anodization period has a significant impact on the process of TNTs production. If the anodization period is too short, there are no TNTs. TNTs may be generated in as little as 15 minutes, and highly organized TNTs can be produced with more time. Similarly, after 5 minutes of anodization, only a nanopores structure was created, and the nanotubular structure was only apparent after 10–20 minutes. Short and narrow TNTs may be readily produced (i.e., 5-min anodization time). The length of TNTs has been enhanced by prolonging the anodization time (Li, et al., 2014). The optimum anodization time with 20 V for the up-scale reactor was 4 hours.

4.2.6 Temperature

At temperatures of 0, 20, and 40 degrees Celsius, self-organized nanotubes emerge in a glycerol electrolyte. Only unstable bundles of tubes may develop on the Ti surface at temperatures over 40°C, and no stable and mechanically stable nanotubular structure can be created. At 5°C, a thick porous oxide layer was formed. At 10°C, a

porous structure with irregularly ordered pores rather than commonly ordered holes was apparent, and at 15°C, regular pores were generated, with pore diameters in the range of 45–50 nm. In addition, two to three additional tiny holes are formed within the old pores. As the temperature rises, well-ordered pores with a diameter of 84 nm emerge (K. Indira, S. Ningshen, Mudali, & N. Rajendran, 2011). Because the anodization time was set to 4 hours, the temperature can be maintained at 20°C.

4.3 Schematic Diagram for Up Scale Reactor

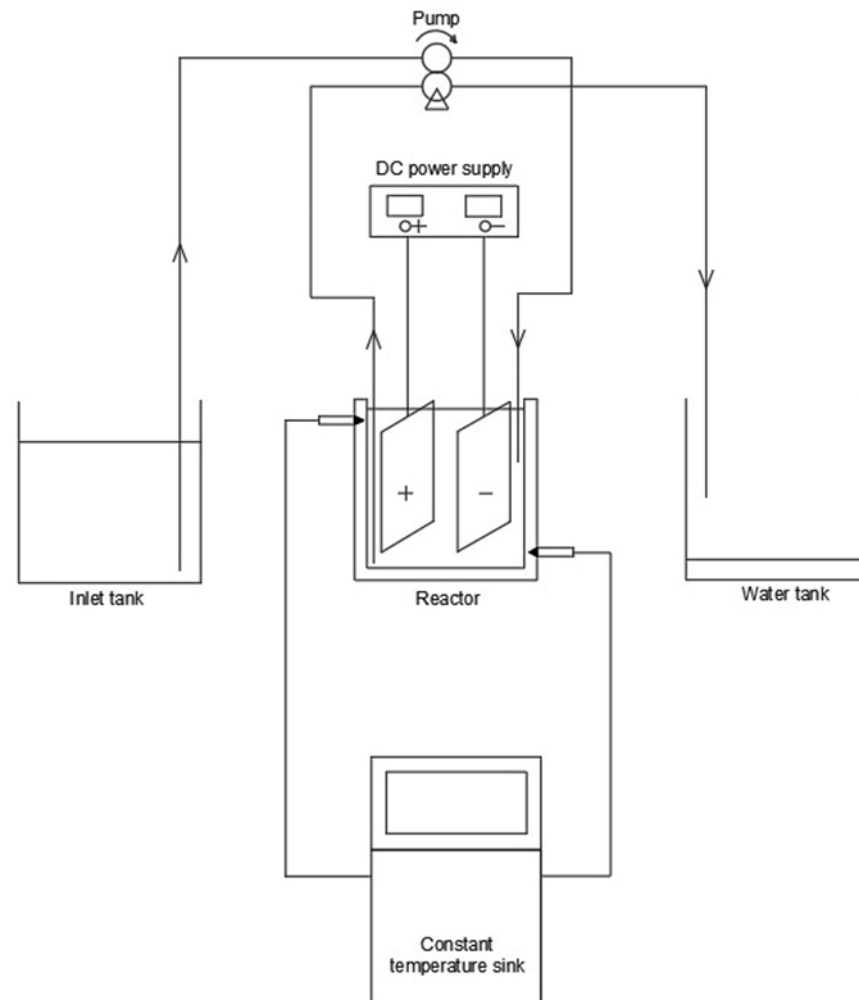


Figure 4.1 Up-scale schematic diagram

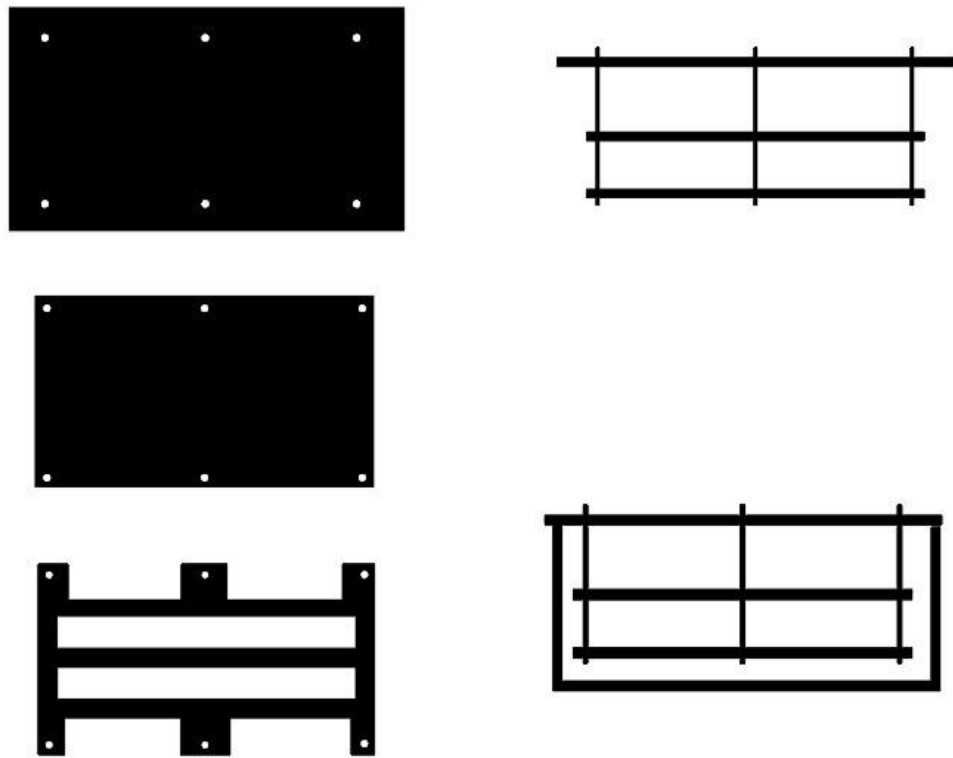


Figure 4.2 Electrode rack design

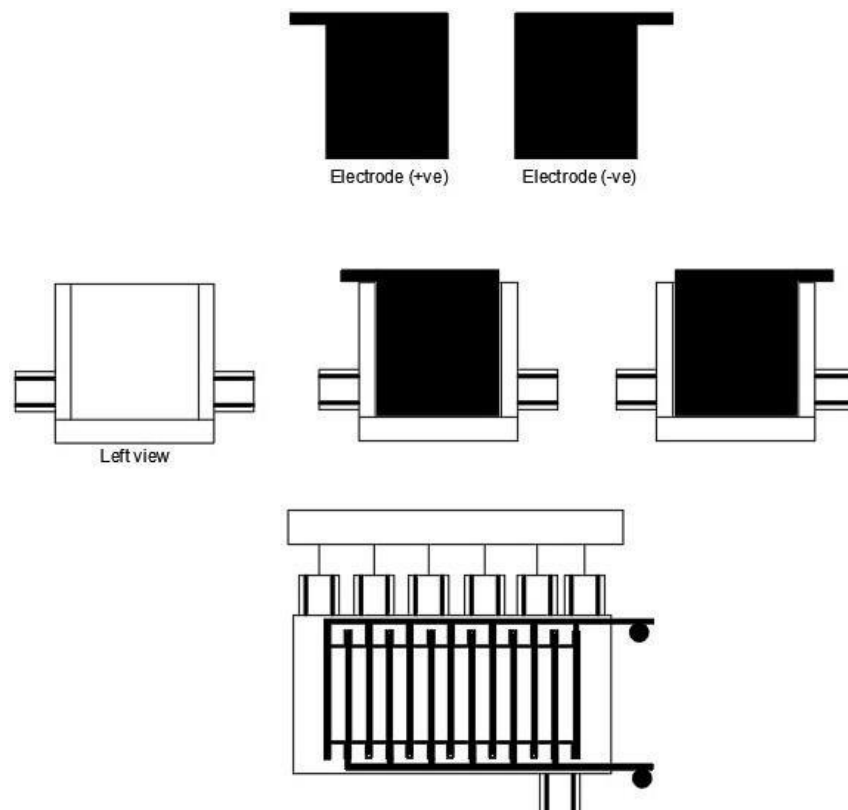


Figure 4.3 Reactor tank design

CHAPTER 5

CONCLUSION

5.1 Conclusion

The reactor is three times larger and more advanced than the previous design, and the reactor rack tank will create more TNTs as a finished product. This scaling-up reactor was used to successfully perform a photocatalytic conversion experiment using CO₂, synthesized photocatalyst in a built gas-solid phase reactor, which would create more and larger size TNTs at the same time while lowering time. TNTs were successfully generated, and the prepared catalysts were characterized using FESEM, EDX, and Cryo-TEM. The results indicated that all of the samples had high catalytic capability features, and they were then carefully selected for further photocatalytic evaluation.

5.2 Recommendation

For future recommendations, the TNTs products need to be tested with the size and length of the nanopores structure created with the up-scale reactor. Some adjustments of the fabrication factor need to take place for the larger size of the reactor.

REFERENCES

- A. M., L. Z., B. C., & J. Y. (2019). Dual Cocatalysts in TiO₂ Photocatalysis. *Advanced Materials*.
- AICHE. (2010, 11 9). *Photocatalytic Activity of TiO₂ and TiO₂-xCxNy Thin Films From Polymer Assisted Deposition*. Retrieved from https://www.aiche.org/academy/videos/conference-presentations/photocatalytic-activity-tio2-and-tio2-xcxny-thin-films-polymer-assisted-deposition?gclid=Cj0KCQjw4cOEBhDMARIsAA3XDRhSw9Gh6H3r0Qpy4wmSpMFwE2cGwNh97ygvS5jXxxHsuX2Zw6mdDTYaAoYUEALw_wcB
- Al Jitan, S., Palmisano, G., & Garlisi, C. (2020). Synthesis and Surface Modification of TiO₂-Based Photocatalysts for the Conversion of CO₂. *Catalysts*.
- Ali, S., A. R., & S.-I. I. (2019). Development of graphene-based photocatalysts for CO₂ reduction to C₁ chemicals: A brief overview. *Catalysis Today*, 39-54.
- Aluminum Anodizers Council. (2017). *What is Anodizing?* Retrieved from ANODIZING... THE FINISH OF CHOICE: <https://www.anodizing.org/page/what-is-anodizing#:~:text=Anodizing%20is%20an%20electrochemical%20process,%2Dresistant%2C%20anodic%20oxide%20finish.&text=Anodizing%20is%20accomplished%20by%20immersing,electric%20current%20through%20the%20medium>.
- Amanda MacMillan Jeff Turrentine. (2021). Global Warming 101.
- Bierwirth, P. (2021). a major unapprehended risk for human health a major unapprehended risk for human health. *Carbon dioxide toxicity and climate change*.
- Bilen, K., O. O., Bakirci, K., S. K., Erdogan, S., M. Y., & O. C. (2007). Energy production, consumption, and environmental pollution for sustainable development: A case study in Turkey. *Renewable and Sustainable Energy*.
- Bin Zhang, M. W. (2012). Fabrication and Characterization of LaF₃/Titania Nanotube Array Electrode for Determination of Fluoride Using a Headspace Single-Drop Microextraction System. *Analytical Letters* , 2455-2466 .

- C. C., C. T., N. F., N. S., M. R., M. M., & Y. A. (n.d.). FIELD EMISSION SCANNING ELECTRON MICROSCOPE (FE-SEM) FACILITY IN BTI. *KEMUDAHAN MIKROSKOP ELEKTRON IMBASAN PANCARAN MEDAN DI BTI*.
- Chao Peng, G. R. (2017). Perspective. *Photocatalytic reduction of CO₂ to solar fuels over semiconductors*.
- Corrosionpedia. (2018, August 3). *What Does Electrolyte Mean?* Retrieved from Electrolyte: <https://www.corrosionpedia.com/definition/440/electrolyte-corrosion>
- D. Pathinettam Padiyan, D. H. (2012). Synthesis of Various Generations Titania Nanotube Arrays by. *EMRS 2011 Spring Meeting*, 88-100.
- D. Shi, Y. F. (2004). Photocatalytic conversion of CH₄ and CO₂ to oxygenated compounds over Cu/CdS–TiO₂/SiO₂ catalyst. *Catalysis Today*, 98 (4) , 505-509.
- Dhinasekaran, D., Rakkesh, R., Saravanan R, & Mu. Naushad. (2020). Principles and Mechanisms of Green Photocatalysis. *Green Photocatalysts*.
- EPA. (2020, DECEMBER 4). *Sources of Greenhouse Gas Emissions*. Retrieved from epa.gov: <https://www.epa.gov/ghgemissions/sources-greenhouse-gas-emissions>
- Erdogan Alper, O. Y. (2017). CO₂ utilization: Developments in conversion processes. *Petroleum*, 109-126.
- F. K. (2020). PHOTOCATALYTIC CONVERSION OF CARBON DIOXIDE TO METHANE USING RGO/Au-TNTs.
- Gang Li, Z. L. (2009). Preparation of Titania Nanotube Arrays by the Hydrothermal Method. *Chinese Journal of Catalysis* , 37-42.
- Gong, D., Grimes, C. A., Varghese, O. K., Hu, W., R. S. Singh, Chen, Z., & Dickey, E. C. (2011). Titanium oxide nanotube arrays prepared by anodic oxidation. *Journal of Materials Research*, 3331–3334.
- H. S., M. B., M. K., R. Z., J. P., J. K., & J. M. (2018). Scaling up anodic TiO₂ nanotube layers for gas phase photocatalysis. *Electrochemistry Communications*, 91-95.
- H. Yin, H. L. (2010). The large diameter and fast growth of self-organized TiO₂ nanotube arrays achieved via electrochemical anodization. *Nanotechnology*, vol. 21.

- Hailemariam, A. (2019). Evidence from Energy Use Evidence from Energy Use. *Carbon Emissions and Public Health*.
- Hanna Sopha , Michal Baudys , Milos Krbal , Raul Zazpe , Jan Prikryl , Josef Krysa , & Jan M.Macak . (2018). Scaling up anodic TiO₂ nanotube layers for gas phase photocatalysis. *Electrochemistry Communications*, 91-95.
- Holly Shaftel, Randal Jackson, Susan Callery & Daniel Bailey. (2021). Carbon Dioxide. *Global Climate Change*.
- Honeychurch, K. (2012). Printed thick-film biosensors. *Printed Films*, 366-409.
- Hoyer, P. (1996). Formation of a Titanium Dioxide Nanotube Array. *Langmuir*, 1411–1413.
- I. A., S.-R. K., S.-P. K., & J.-O. K. (2017). Anodization of bismuth doped TiO₂ nanotubes composite for photocatalytic degradation of phenol in visible light. *Catalysis Today*, 31-37.
- Indira, K., Mudali, U. K., & Nishimura, T. (2015). A Review on TiO₂ Nanotubes: Influence of Anodization Parameters, Formation Mechanism, Properties, Corrosion Behavior, and Biomedical Applications. *Journal of Bio- and Tribo-Corrosion*.
- J. G. (2000). CHAPTER 1 - ELECTROCHEMICAL OXIDATION AND REDUCTION OF ORGANIC COMPOUNDS. *Electrochemical Reactions and Mechanisms in Organic Chemistry*, 1-26.
- J. H., K. Z., & Y. L. (2015). Recent Advances in Preparation, Modification and Applications of TiO₂ Nanostructures by Electrochemical Anodization. *Handbook of Nanoelectrochemistry*.
- J. L., B. C., & J. Y. (2017). Surface modification and enhanced photocatalytic CO₂ reduction performance of TiO₂: a review. *Applied Surface Science*, 658-686.
- J. Y., G. D., & B. C. (2010). Effect of Crystallization Methods on Morphology and Photocatalytic Activity of Anodized TiO₂ Nanotube Array Films. *The Journal of Physical Chemistry C*.
- J.-Y. H., K.-Q. Z., & Y.-K. L. (2013). TiO₂ Nanotube Arrays by Electrochemical Synthesis: A Review. *Fabrication, Modification, and Emerging Applications*.

- John Moma, Jeffrey Baloyi. (2018). Modified Titanium Dioxide for Photocatalytic Applications.
- K. Indira, S. Ningshen, Mudali, U., & N. Rajendran. (2011). Effect of Anodization Temperature on the Surface Morphology of Anodized Titanium. 63–66.
- K. Indira, U. K. (2015). Review on TiO₂ Nanotubes: Influence of Anodization Parameters, Formation Mechanism, Properties, Corrosion Behavior, and Biomedical Applications. *Journal of Bio- and Tribo-Corrosion*.
- K. K., B. A., M. R.-G., & J. M. (2020). Photocatalytic activity and smartness of TiO₂ nanotube arrays for room temperature acetone sensing. *Journal of Molecular Liquids*.
- K. W., Y. L., J. H., L. X., L. Y., Y. J., . . . J. N. (2020). Insights into electrochemical decomposition mechanism of lipopolysaccharide using TiO₂ nanotubes arrays electrode. *Journal of Hazardous Materials*.
- Khan, A. A., & M. T. (2019). Recent advancements in engineering approach towards design of photo-reactors for selective photocatalytic CO₂ reduction to renewable fuels. *Journal of CO₂ Utilization*, 205-239.
- KHANI, M. (2017). PHOTOCATALYTIC REDUCTION OF CARBON DIOXIDE AND METHANE.
- KHATUN, F. (2020). PHOTOCATALYTIC CONVERSION OF CARBON DIOXIDE TO METHANE USING.
- Kim, D., Fujimoto, S., Schmuki, P., & Tsuchiya, H. (2008). Nitrogen doped anodic TiO₂ nanotubes grown from nitrogen-containing Ti alloys. *Electrochemistry Communications*, 910-913.
- Kočí, K., Obalová, L., & Lacný, Z. (2007). Photocatalytic reduction of CO₂ over TiO₂ based catalysts.
- Kumar, A., Thakur, P. R., Sharma, G., M. N., Rana, A., Mola, G. T., & Stadler, F. J. (2019). Carbon nitride, metal nitrides, phosphides, chalcogenides, perovskites and carbides nanophotocatalysts for environmental applications. *Environmental Chemistry Letters*, 655-682.

- Li, K., Peng, B., & Peng, T. (2016). Recent Advances in Heterogeneous Photocatalytic CO₂ Conversion to Solar Fuels. *Catalysis*.
- Li, Y., Ma, Q., Han, J., Ji, L., Wang, J., Chen, J., & Wang, Y. (2014). Controllable preparation, growth mechanism and the properties research of TiO₂ nanotube arrays. *Applied Surface Science*, 103-108.
- Liu, X. & (2017). CO₂ seasonal variation and global change. *Test global warming from another point of view*.
- M. Humayun, F. Raiq, A. Khan, & W. Luo. (2018). Modification strategies of TiO₂ for potential applications in photocatalysis: a critical review. *Green Chemistry Letters and Reviews* , 86-102.
- M. P., S. T., & P. G. (2018). A Brief Overview of TiO₂ Photocatalyst for Organic Dye Remediation: Case Study of Reaction Mechanisms Involved in Ce-TiO₂ Photocatalysts System. *Nanomaterials*.
- M. S., S. B., R. B., H. K., & E. B. (2018). Energy Dispersive X-ray (EDX) microanalysis: A powerful tool in biomedical research and diagnosis. *European journal of histochemistry: EJH*.
- Márk Szuhaj, Norbert Ács, Roland Tengölics, Attila Bodor, Gábor Rákhely, Kornél L. Kovács, & Zoltán Bagi. (2016). Conversion of H₂ and CO₂ to CH₄ and acetate in fed-batch biogas reactors by mixed biogas community: a novel route for the power-to-gas concept. *Biotechnology for Biofuels*.
- N. D., & R. L. (2013). Cryogenic Transmission Electron Microscopy: Aqueous Suspensions of Nanoscale Objects. *Microscopy and Microanalysis*.
- N. T., R. N., C. F., S. L., & M. H. (2020). Visible Light Photodegradation of Formaldehyde over TiO₂ Nanotubes Synthesized via Electrochemical Anodization of Titanium Foil. *nanomaterials*.
- Neda Yazdanpour, S. S. (2013). Solar Energy Materials and Solar Cells. *Photocatalytic conversion of greenhouse gases (CO₂ and CH₄) using copper phthalocyanine modified TiO₂*, 1-8.
- Ochedi, F. O., Liu, D., Yu, J., Hussain, A., & Liu, Y. (2020). Photocatalytic, electrocatalytic and photoelectrocatalytic conversion of carbon dioxide: a review. *Environmental Chemistry Letters*, 941-967.

- OECD GREEN GROWTH STUDIES. (2011). Energy.
- P. M., W. L., T. G., Winiarski, M. J., T. K., A. M., . . . J. N. (2017). Enhanced photocatalytic properties of lanthanide-TiO₂ nanotubes: An experimental and theoretical study. *Applied Catalysis B: Environmental*, 376-385.
- Papadaki, D. G. (2017). Environmental performance of photocatalytic materials for energy save. *Environmental behavior of photocatalytic materials, with the aim of saving energy*.
- Planton, & Serge. (2013). *Annex III: Glossary*. Cambridge University Press, Cambridge, United Kingdom and New York, NY, USA.: IPCC, 2013.
- Powell, J. (2019). Scientists Reach 100% Consensus on Anthropogenic Global Warming. *Bulletin of Science, Technology and Society*.
- R. Beranek, H. H. (2003). Self-organized porous titanium oxide prepared in H₂SO₄/HF electrolytes,. *Electrochemical and Solid-State Letters*, B12–B14.
- R. Hahn, J. M. (2007). Rapid anodic growth of TiO₂ and WO₃ nanotubes in fluoride free electrolytes. *Electrochemistry Communications*, 947–952.
- R. L., & C. L. (2017). Chapter One - Photocatalytic Water Splitting on Semiconductor-Based Photocatalysts. *Advances in Catalysis*, 1-57.
- Ribeiro, B., Offoiach, R., Rahimi, E., Salatin, E., Lekka, M., & Fedrizzi, L. (2021). Influence of Microstructure and Anodization Parameters. *On Growth and Morphology of TiO₂ Nanotubes on Ti6Al4V by Anodic Oxidation in Ethylene Glycol Electrolyte*.
- Schmuki, S. P. (2010). TiO₂ nanotubes grown in different organic electrolytes: two-size self-organization, single vs. double-walled tubes, and giant diameters. *Physica Status Solidi*, 15–217.
- Shahram Sharifnia, & Yazdanpour Neda. (2013). Photocatalytic conversion of greenhouse gases (CO₂ and CH₄) using copper phthalocyanine modified TiO₂. *Solar Energy Materials and Solar Cells*.
- Shehzad, N., M. T., Johari, K., Murugesan, T., & Hussain, M. (2018). A critical review on TiO₂ based photocatalytic CO₂ reduction system: Strategies to improve efficiency. *Journal of CO₂ Utilization*, 98-122.

- T. A., C. M., R. K., S. K., & B. S. (2019). Electrochemical Performance of Nitrogen-Doped TiO₂ Nanotubes as Electrode Material for Supercapacitor and Li-Ion Battery. *Advanced Materials for Solar Energy*.
- T. T., J. S., B. P., K. P., D. S., & J. S. (2018). Structural modulation and band gap optimisation of electrochemically anodised TiO₂ nanotubes. *Materials Science in Semiconductor Processing*, 150-158.
- W. K., S. S., A.-F. M., N. N., G. K., H. M., & A. M. (2013). Low-temperature crystallization of TiO₂ nanotube arrays via hot water treatment and their photocatalytic properties under visible-light irradiation. *Materials Chemistry and Physics*, 991-998.
- Xie, S., Zhang, Q., Liu, G., & Wang, Y. (2016). Photocatalytic and photoelectrocatalytic reduction of CO₂ using heterogeneous catalysts with controlled nanostructures. *Chemical communications*.
- Y. C., Y. W., W. L., Q. Y., Q. H., L. W., . . . M. J. (2017). Enhancement of photocatalytic performance with the use of noble-metal-decorated TiO₂ nanocrystals as highly active catalysts for aerobic oxidation under visible-light irradiation. *Applied Catalysis B: Environmental*, 352-367.
- Yang, G., Chen, D., Ding, H., FengFeng, J., Zhang, J. Z., Zhu, Y., . . . Bahnemann, D. W. (2019). Well-designed 3D ZnIn₂S₄ nanosheets/TiO₂ nanobelts as direct Z-scheme photocatalysts for CO₂ photoreduction into renewable hydrocarbon fuel with high efficiency. *Applied Catalysis B: Environmental*, 611-618.
- Yi , X., Zhiliang , M., Wei , S., Qunhui , W., Xiaona , W., & Hui , Z. (2020). Analysis of Research Status of CO₂ Conversion Technology Based on Bibliometrics. *Catalysts*.
- Yin Yea, H. B. (2019). Effect of dissolved natural organic matter on the photocatalytic micropollutant removal performance of TiO₂ nanotube array. *Journal of Photochemistry and Photobiology A: Chemistry*, 216-222.
- Z. P., Z. S., J. C., W. L., J. C., Y. L., & K. C. (2020). Enhanced charge generation and transfer performance of the conical bamboo-like TiO₂ nanotube arrays photo-electrodes in quantum dot sensitized solar cells. *Solar Energy*, 161 - 169.
- Z. Y., Y. Z., H. W., X. C., Y. F., H. Y., . . . P. W. (2019). Synthesis, surface properties, crystal structure and dye-sensitized solar cell performance of TiO₂ nanotube arrays anodized under different parameters. *Results in Physics*.

Z.-C. G., H.-P. W., X. W., J. H., & R.-G. D. (2018). Fabrication of heterostructured β -Bi₂O₃-TiO₂ nanotube array composite film for photoelectrochemical cathodic protection applications. *Corrosion Science*, 60-69.

APPENDICES